Lara Strohmeier, BSc

Developement of thiol based resins for the 3D printing of biocompatible composite structures

MASTER'S THESIS

to achieve the university degree of

Diplom-Ingenieurin

Master's degree programme: Technical Chemistry

submitted to

Graz University of Technology

Supervisor

Assoc.Prof. Dipl.-Ing. Dr.techn. Gregor Trimmel

Institute for Chemistry and Technology of Materials

Graz, July 2018

AFFIDAVIT

I declare that I have authored this thesis independently, that I have not used other than the declared sources/resources, and that I have explicitly indicated all material which has been quoted either literally or by content from the sources used. The text document uploaded to TUGRAZonline is identical to the present master‘s thesis.

Date

Signature

Abstract

The aim of this master thesis is the investigation of a ternary methacrylate-thiol-yne system which can be used as binding material for ceramic particles to realize 3D-printed composite structures as well as high-performance ceramics.

The main advantage of such a ternary system is the higher monomer conversion of the methacrylate compared to pure methacrylate systems. Additionally, sole methacrylate systems are known for their cytotoxicity and skin irritating properties. The ternary system should overcome the drawbacks of pure methacrylate systems to yield a biocompatible polymer for medical applications.

Firstly, a suitable ternary system was developed and investigated concerning its storage stability and photo reactivity. The reaction rate of the formulations was determined using photo-differential scanning calorimetry (DSC) and the monomer conversion was analysed through real-time Fourier-transform infrared spectroscopy (FTIR). The migration of remaining monomers out of the cured resin was determined via gas chromatography-mass spectrometry (GC-MS) measurements. The mechanical properties of the cured resins were investigated via a charpy-impact test and its heat deflection temperature (HDT). Finally, the 3D-printing ability of the resin was tested.

Finally, the ternary resin was blended with two different fillers, e.g. tricalcium phosphate (TCP) and alumina oxide (Al_2O_3). The maximum degree of filling and the behaviour of the filled resins regarding their storage stability was evaluated.

It was possible to obtain an efficient stabilizer system for an improved shelf-life of the ternary resins. Furthermore, the Photo-DSC analysis of the ternary systems showed a fast reaction rate as well as a high monomer conversion.

Due to the high monomer conversion no significant migration of the monomers was detected with the GC-MS analysis of the polymers. Also, the ternary system exhibited advanced mechanical properties compared to a pure methacrylate system. Furthermore, a high heat deflection temperature (HDT) was determined.

The 3D-printing tests of the ternary resin were successful and defined bone-screws could be obtained. Finally, it was possible to fill the ternary system with up to 65 wt% of ceramic particles.

The benefits of the developed ternary system include a high monomer conversion and improved mechanical properties compared to pure methacrylate systems. Since a good 3D-printing ability was demonstrated successfully, the newly developed ternary system is a suitable substitution for pure methacrylate system.

Acknowledgement

First of all, I would like to thank my supervisors Prof. Gregor Trimmel from the TU Graz and Prof. Thomas Griesser from the Montanuniversität Leoben who enabled this joint master thesis. Also, a big thanks to Lithoz for providing this interesting research topic. Furthermore, I would also like to thank Daniel Hennen for his advice and support along the way.

I would like to thank my fellow colleagues from the Christian Doppler Laboratory (CDL) for the feedback, support and, of course, the pleasant working environment.

A special thanks to the Christian Doppler Research Association for their financial support, which was greatly appreciated.

Also, I would like to thank my boyfriend René for his constant support and his encouragement to keep going. I also want to thank my fellow colleagues for their company and their friendship throughout the last years.

Last but not least I want to thank my parents, Helmut and Sibylle, who made everything possible. Thank you for the emotional and – of course - financial support throughout the years.

LITHOZ

NAWI Graz
Natural Sciences

Table of content

1. Motivation and outline

A high interest in the development of biocompatible, UV curable resins for medical application has occurred over the past years.[1] This is due to the increasing employment of additive manufacturing in industrial fields in recent years.[2] A variety of technologies for casting different materials (e.g. metals[3,4] ceramics[4,5] and polymers[6,7]) have already been established. Each material offers unique profiles concerning chemical and physical features, but also process behavior and physiological interactions such as biocompatibility and degradability.[8] Of all these materials, polymers appear to be the most suitable class due to their high freedom of design in their molecular structure. In particular, Tailor-made resin systems offer a broad range of properties and can be optimized for their specific field of application.[9]

During the last decade, the lithographic-based additive manufacturing technology has become an important research field for polymeric materials.[10–12] Compared to other 3D-printing methods, this technique offers numerous advantages, including a higher writing speed and a better solution.[13] With the lithographic-based additive manufacturing, photopolymerizable resins filled with ceramic particles can be processed for medical usage. After UV-curing, an organic matrix filled with ceramic particles is obtained. This composite can then undergo a thermal treatment step at 600 °C to remove the organic backbone and, after a following sintering, a dense ceramic material is received. Since shrinkage stress of the polymeric binder material can cause problems during the sintering step, a resin with a low shrinkage stress is required. The final materials can be used for customized bone replacement or scaffolds in the medial sector.[12]

For example, the obtained ceramic materials can be used for internal fixation, a method to support and position fractured bones without leaving an open wound.[14] Normally, the used devices are mainly made of metal and can hinder the bone growth, in which case a second surgery is required to remove the fixation.[15] To overcome this problem, biodegradable polymers have been developed which can be metabolized and cleared from the body.[16,17]

However, one major drawback of these polymers is their radiolucent behavior.[18] This means that it is not possible to monitor the device using x-ray imaging. With the addition of ceramic particles a radiopaque composite material is created. Furthermore, composite and pure ceramic materials offer better mechanical properties and higher strength.[19]

The most common resins in lithographic processes consist of multifunctional acrylates and methacrylates since they feature many desirable properties like fast curing and no requirement for solvents.[20]. The high curing rates are caused by a fast radical chain growth polymerization which yields highly-crosslinked networks within seconds.[10] During the polymerization, the gelation point is reached very quickly and leads to a limited (meth)acrylate conversion, which does not exceed 60-90%. Due to the early vitrification, the mobility of the monomers is limited and a complete (meth)acrylate conversion is not possible.[21] The resulting residual monomers within the network can migrate from the cured polymer. The migration of these monomers is responsible for high irritancy potential and cytotoxicity due to their function as Michael acceptors, which can cause reactions with amino- or thiol-groups of proteins or DNA molecules.[22–24] Therefore, the usability of (meth)acrylate resins in biomedical applications is limited.[23,24] However, in comparison to acrylates, methacrylates show a lower cytotoxicity which makes them suitable for 3D- printing devices used in the dental section.[25] Furthermore, (meth)acrylate resins experience a high shrinkage stress during the curing process that leads to brittle materials.[9,10,26]

The photoreactive thiol-ene and thiol-yne systems, which have been explored in recent years, can serve as possible replacements for (meth)acrylate resins.[21,27,28] These systems feature a step-growth mechanism leading to a delayed gelation point compared to (meth)acrylates. This step-growth mechanism yields an increased monomer mobility for an extended amount of time while the curing reaction takes place, resulting in a higher overall monomer conversion.[21] This enhanced conversion of this reaction type limits the migration of monomers to a minimum, which leads to a high biocompatibility. Moreover, the internal shrinkage stress is reduced due to the delayed gelation point which enables the usage of tougher materials.[27,29,30] However, one drawback of the delayed gel point is the reduced printability of the thiol-ene and thiol-yne systems.

To combine the fast curing speed of (meth)acrylates and the higher monomer conversion of thiol-yne systems, ternary (meth)acrylate-thiol-yne systems were developed by Bowman et al.[31] Due to the fast chain-growth homopolymerization of the (meth)acrylates, the gelpoint occurs at an earlier state of the polymerization compared to a pure thiol-yne system but it also shows a delayed gel point compared to a pure (meth)acrylate system. This leads to an improvement of the printability compared to sole thiol-yne systems. The homopolymerization of the double bonds is accompanied by a chain transfer to the thiol and thiol-ene step growth mechanism. This leads to a homogeneous and highly cross-linked resin which exhibits a high monomer conversion due to the step-growth mechanism. Due to the higher monomer conversion, the ternary systems is predicted to offer a higher biocompatibility and lower cytotoxicity accompanied by a faster curing speed and higher toughness.[31,32]

The aim of this master thesis was to investigate a suitable thiol-yne-methacrylate system for 3D-printable medical devices. In the first approach the ternary system was studied concerning its storage stability, photo reactivity and monomer conversion. Additionally, the resin was evaluated towards its possible utilization in composite materials and printable high-performance ceramics.

2. Introduction

2.1. Materials for photopolymerization

2.1.1. Chain growth polymerization of (meth)acrylate resins

In Scheme 1 the radical chain-growth polymerization of (meth)acrylates is illustrated. In photo-curable resins the free radicals are generated through a light sensitive photoinitiator. These radicals are able to attack a carbon-carbon double bond with subsequent formation of a carbon centered radical, which is capable of starting the next propagation step. During the formation of the covalent bonds in the cross-linking networks, the free volume is reduced and yields the shrinkage stress responsible for brittle materials.[33]

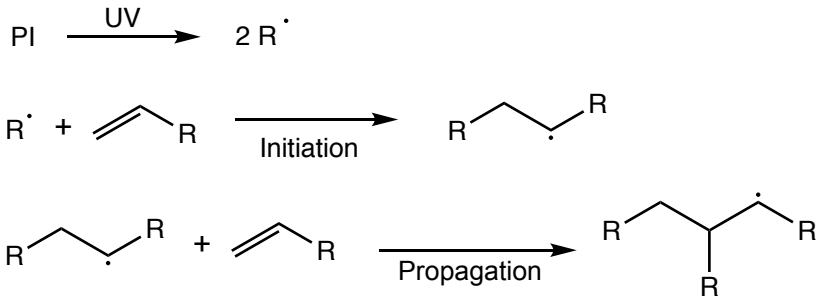

Scheme 1 Radical mediated, photo induced chain-growth mechanism.

Since the gelation point is reached very fast in this process, the (meth)acrylate conversion is not exceeding 60-90%. The mobility of the monomers is limited and they are thus unable to find a reactive counterpart due to the early vitrification. This leads to residual monomers within the network which can migrate from the cured polymer.

2.1.2. Thiol-ene and thiol-yne step-growth polymerization

The thiol-ene reaction proceeds via a radical mediated step-growth polymerization. This reaction mechanism has been demonstrated to reduce the shrinkage stress by delaying the gelation during the polymerization.[29] The step-growth polymerization consists of alternating addition and chain transfer reactions, which results in a slow and uniform network formation that causes the delayed gelation and, therefore, a reduced shrinkage stress.

Further advantages of the thiol-ene polymerization reaction include high selectivity, high yield with minimal side reactions, and little sensitivity against oxygen or moisture. Two major

drawbacks of the thiol-ene polymerization reaction are the distinct odor of the thiols and the rather low storage stability of thiol-ene compounds.[30]

Also, the crosslink-density for thiol-ene polymers is lower compared to pure (meth)acrylate polymers. Depending on the mechanism, the vinyl group is capable of acting as either a mono- or difunctional moiety. The (meth)acrylate polymerization proceeds via a chain-growth mechanism leading to a replacement of each carbon-carbon double bond by two single bonds. In contrast to this, the thiol-ene polymerization leads to the conversion of a vinyl to a single thioether which establishes the vinyl group as monofunctional.[34] This limits the ultimate crosslinking-density in materials that causes a decreased glass transition temperature (T_g). This poses severe limitations for this material class.[35]

In Scheme 2 the reaction path of a thiol-ene polymerization reaction is displayed. At first, a free radical is created through the illumination of a photoinitiator. This free radical can abstract a hydrogen atom from the thiol to generate a thiyl radical, which then adds to a carbon-carbon double bond to yield a carbon centered radical. This radical subsequently substracts a hydrogen from another thiol functional group which generates another thiyl radical. [36]

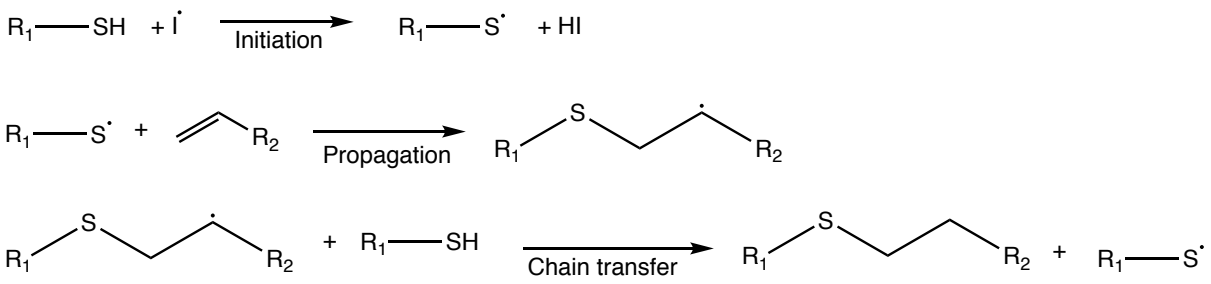

Scheme 2 Radical mediated thiol-ene step-growth polymerization.

Thiol-yne polymerization reactions have also been demonstrated to follow a radical step-growth polymerization mechanism. The reaction path of the thiol-yne polymerization is depicted in Scheme 3.

Similar to the thiol-ene polymerization reaction, a thiyl radical is generated due to light induced photoinitiation. This free radical can react with the carbon-carbon triple bond to yield a carbon-centered radical. Subsequently this radical abstracts a hydrogen from a thiol functional group. This leads to the formation of a vinyl sulfide moiety capable of reacting with

another thiol monomer according to the thiol-ene polymerization reaction mechanism mentioned above.

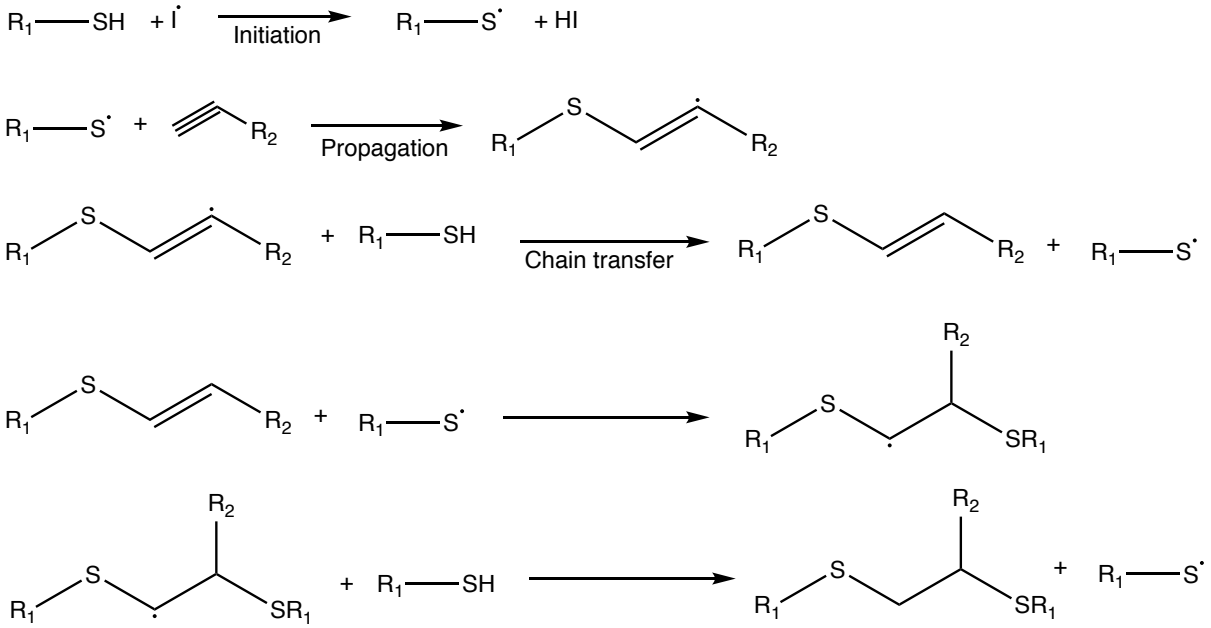

Scheme 3 Radical mediated thiol-yne step-growth polymerization.

Since each alkyne group reacts with a thiyl radical twice, a higher cross-link density in the polymer is achieved. This leads to a higher T_g and advanced mechanical properties compared to the thiol-ene reaction. [34,37,38]

2.1.3. Properties of ternary systems

Ternary photo-polymerizable systems enable the combination of the fast chain growth mechanism of (meth)acrylates with the step growth mechanism of thiol-yne and thiol-ene systems.[31] With such ternary systems, unique reaction kinetics (see Figure 1) and network formation are created and it is possible to directly tailor the network material properties. Due to the arising competition between the (meth)acrylate homopolymerization and the chain transfer to a thiol, a thiol-ene or thiol-yne step growth polymerization is promoted.[32]

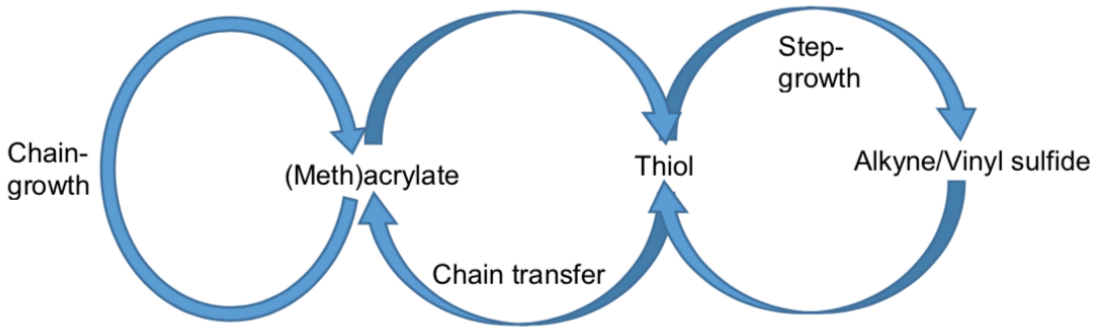

Figure 1 Competition between chain-growth, chain transfer and step-growth mechanism in a thiol-yne-(meth)acrylate ternary system.[31]

By varying the stoichiometric ratio and structure of the monomers in the ternary system, the T_g and homogeniety of the network can be controlled. This leads to the achievement of tailor-made resins with favorable network properties. Thus, the gelation point of the ternary system can be adjusted with varying ratios of methacrylate to thiol-yne. This has a positive impact on 3D-printing abilities since a fast curing rate is crucial. In pure thiol-yne systems the delayed gelation of the material causes severe limitations regarding the printing speed and ability. The addition of (meth)acrylates can overcome these problems.

Furthermore, a ternary system was studied by Bowman et al.[33] They observed a significant decrease in shrinkage stress by incorporating a thiol-allyl ether or alkyne[31] into a methacrylate system. During the polymerization the methacrylate domains reach higher conversions while the thiol-ene and thiol-yne regimes are still consisting of small oligomers with enough mobility to act as plasticizing solvent during the early stages. The internal stresses during the vitrification are at a comparable rate to thiol-ene systems. This combination of materials can reduce the methacrylate shrinkage stress up to 50% while maintaining a high T_g.[33] The formation of the network evolution are shown in Scheme 4.

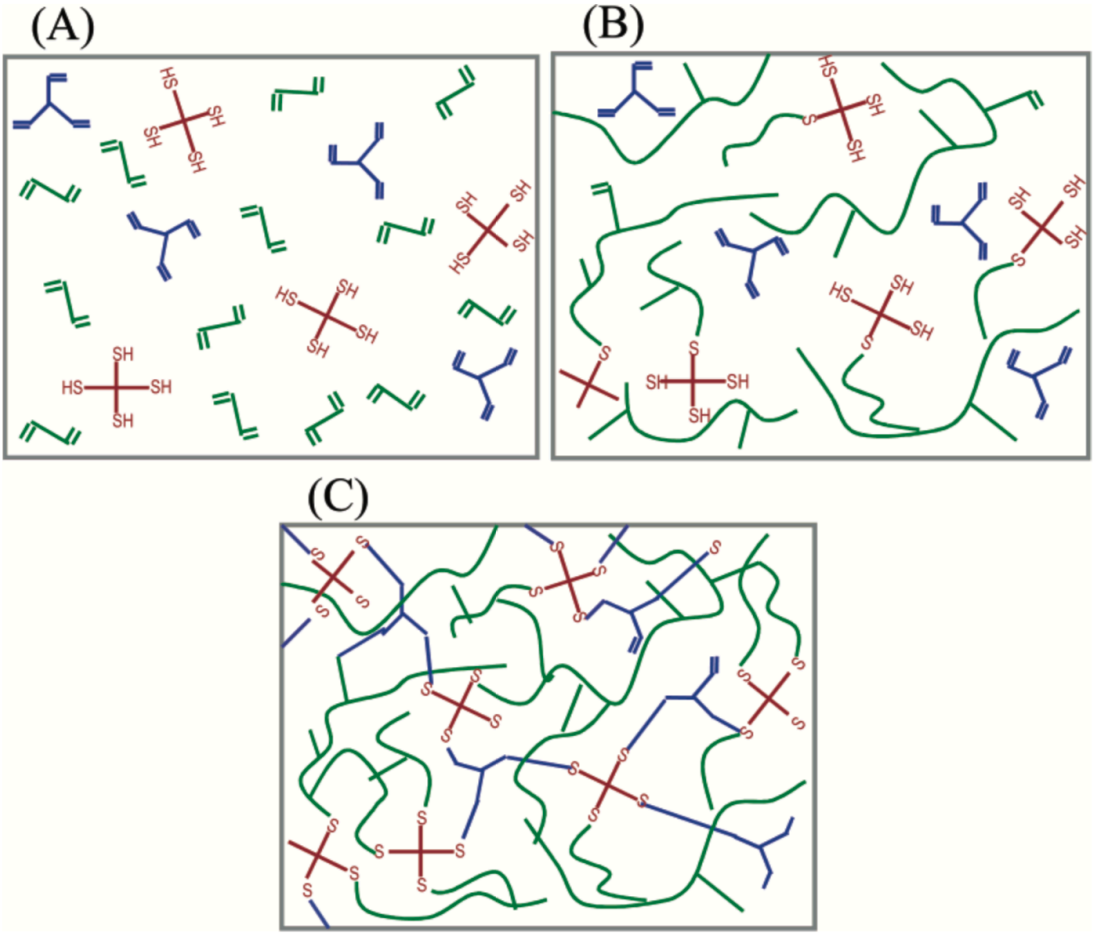

Scheme 4 Network evolution of a thiol-ene-methacrylate systeme: (A) Before polymerization (B) formation of methacrylate domains (C) formation of thiol-ene domains.[33]

Thiol-yne-methacrylate systems were demonstrated to achieve high T_g and moduli while maintaining low shrinkage stress. These low levels of shrinkage stress were maintained as the thiol-yne component comprises a delayed gelation. Since a large portion of shrinkage takes place before the gel point is reached, most stresses can be released instead of being stored within the solid network.[31]

2.1.4. Stabilizer systems for increased shelf-life storage of resins

One of the major drawbacks of the thiol-ene system is the premature polymerization of the resin at room temperature. Since a long shelf-life stability for industrial applications is required, several stabilizer systems have been proposed to enhance the storage stability.[39,40]

One of the possible reasons responsible for the limited storage stability of thiol-ene systems is a base-induced Michael addition reaction of the thiol groups to the ene double bond. Moreover, hydroperoxides impurities, as well as the generation of radicals through a ground-state charge between thiol and the ene components, can initiate dark polymerization reactions.[41,42]

It was shown that a combined system based on hydroxybenzene compounds with phosphonic acids showed an increased storage stability of thiol-ene formulations compared to the solitary use of radical scavengers.[40] The most efficient radical stabilization in a single stabilizer system was provided by pyrogallol. This is mainly due to the high resonance stabilization of the formed pyrogallol radical caused by intramolecular hydrogen bond interaction.[43] With the combination of a phosphonic acid with pyrogallol the storage stability could be further increased.

However, one major drawback of an efficient stabilizer system is its influence on the reactivity. The Photo-DSC measurements of the stabilized thiol-ene system showed that a higher amount of stabilizers can slightly decrease the photoreactivity.[39,40]

2.2. Additive manufacturing of polymeric materials

Additive manufacturing technologies (AMT) revolutionized the construction of prototypes. Previous prototype manufacturing were performed mechanically. Nowadays, advanced 3D-printing devices are computer-operated and capable of generating three-dimensional prototypes automatically and within a short time.[15]

More recent applications include the 3D printing of medical devices. With help of magnet resonance scan or computer tomography the basis for a three-dimensional implant model can be provided.[44] This 3D model can be digitally customized and a unique CAD model is generated. This technique is capable of decreasing production costs and manufacturing time while creating individualized medical devices. [1,45]

For polymeric materials the stereolithography 3D-printing process became very important.[10–12] The process was discovered in 1980s as a rapid prototyping method for the automotive

industry.[46] In recent years, a variety of AMT have been developed (e.g. selective laser sintering, fused deposition modeling etc.) but stereolithography still delivers the best resolutions while providing incredible freedom of design. Resolutions ranging from 10 µm can be achieved and nearly every geometry can be printed using this technique.

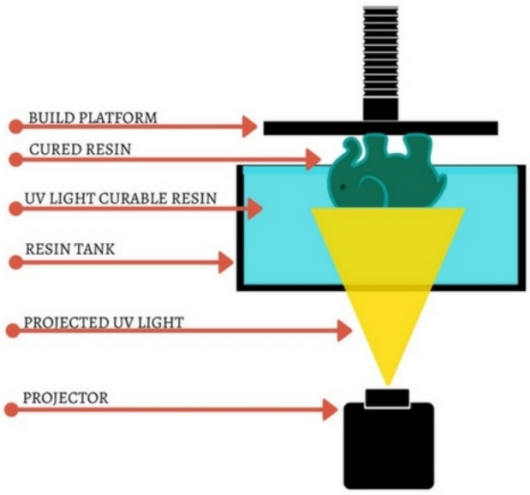

Figure 2 Design of a stereolithography 3D printer.

Figure 2 shows the design of a stereolithography DLP 3D-printing device. The printer consists of a movable platform, a basin filled with the monomer resin, a transparent bottom, and a UV-light source. During the printing process, the platform moves into the resin in a z-axis and stops at a defined height. The residual monomer is suppressed and the resin is illuminated with a UV-light source through the transparent bottom of the basin to yield the first layer of the specimen. The selective curing of one monomer layer can either be carried out by a series of punctual illuminations by a UV-laser beam (direct laser writing) or by a digital light projector (DLP), which illuminates a complete layer of resin at once. Right after the first layer has successfully been solidified, the platform is moved in vertical direction to apply a fresh layer of resin. This process of illumination and vertical movement creates the desired three-dimensional object layer by layer and is repeated until the device is finished. The finished material is then washed to remove excess resin and finally post cured to increase monomer conversion and crosslink density.[47]

2.3. High performance ceramics for medical applications

Tissue engineering is an important field of research in regenerative medicine, especially scaffold based bone repair/regeneration.[48] Damaged bones can be treated with biodegradable three-dimensional scaffolds, which can mimic the extra cellular matrix. They serve as mechanical support or act as a template for cell attachment.[49]

The best way to produce these scaffolds is the additive manufacturing technology which is able to provide structures with tailored porosity and scaffolds for patient specific defects. These individualized components can be manufactured with the data obtained via computer tomography.[50,51] For these medical applications tricalcium phosphate is an appealing material due to its high biocompatibility and structural similarity to natural bone.[49] In Figure 3 a medical device made out of TCP can be seen.

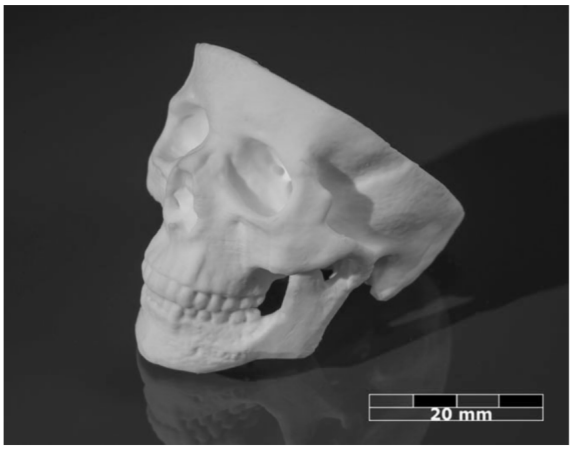

Figure 3 Human skull replica made out of TCP.[52]

The process of the 3D-printing of high performance ceramics is called lithography-based ceramic manufacturing.[53] At first, a photocurable resin is filled with the desired ceramic particles and, afterwards, cured with UV-light to yield a three-dimensional composite object.[54] In a consecutive step, the polymeric backbone is pyrolized[55] and the residual compact is sintered. This last process step is responsible for the final mechanical performance since changes in chemical and/or phase composition can occur. The final product is a dense ceramic material which can be used in various applications.[52] Filled materials have several advantages compared to polymer devices. One of them is the radiopacity of composite and pure ceramic materials which makes the specimen visible in x-ray imaging.[18] Additionally, the mechanical properties are enhanced.[19]

2.4. Photo-Differential Scanning Calorimetry

DSC analysis is used for the fast and simple determination of absorbed or released heat of a sample during the heating, cooling or illumination process. The difference in temperature between a reference and sample crucible is measured to calculate the absorbed or released amount of heat as a function of time and temperature. A basic DSC test setup is shown in Figure 4.

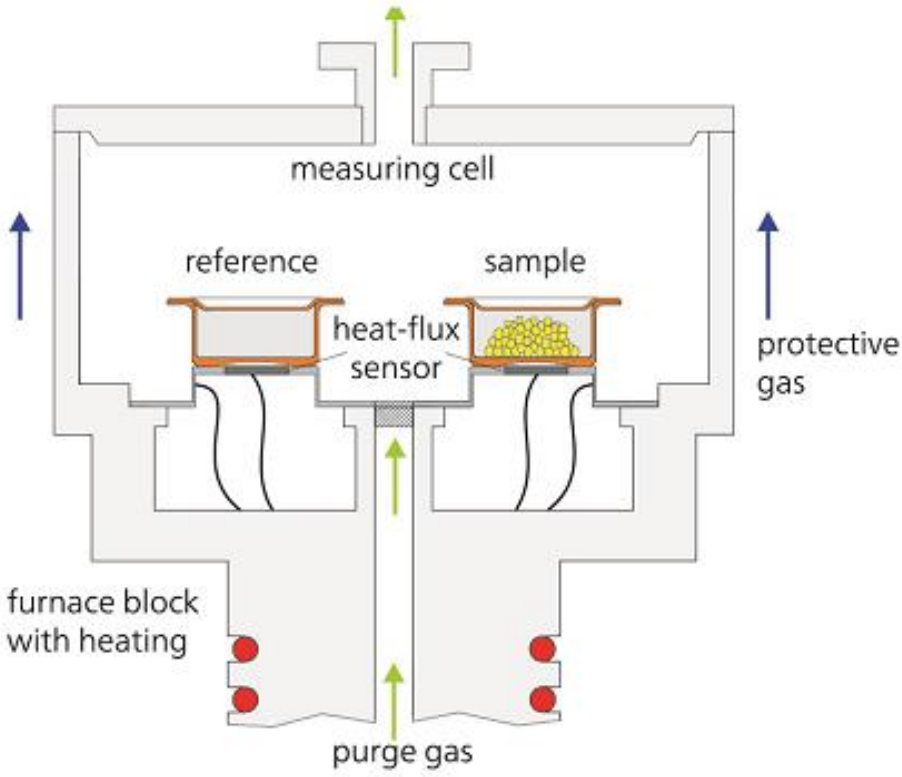

Figure 4 Schematic of a basic DSC test setup.[56]

In a Photo-DSC setup, the temperature of both crucibles is kept constant while the sample is illuminated with UV-light. The released heat of a photopolymerization can then be monitored. As seen in Figure 5, the reaction enthalpy ΔH can be obtained through an integration of the curve. If the theoretical standard enthalpy of reaction ΔH_{th} is known, the monomer conversion (DC) can be estimated according to the following equation.

$$DC = \frac{\Delta H}{\Delta H_{th}}$$

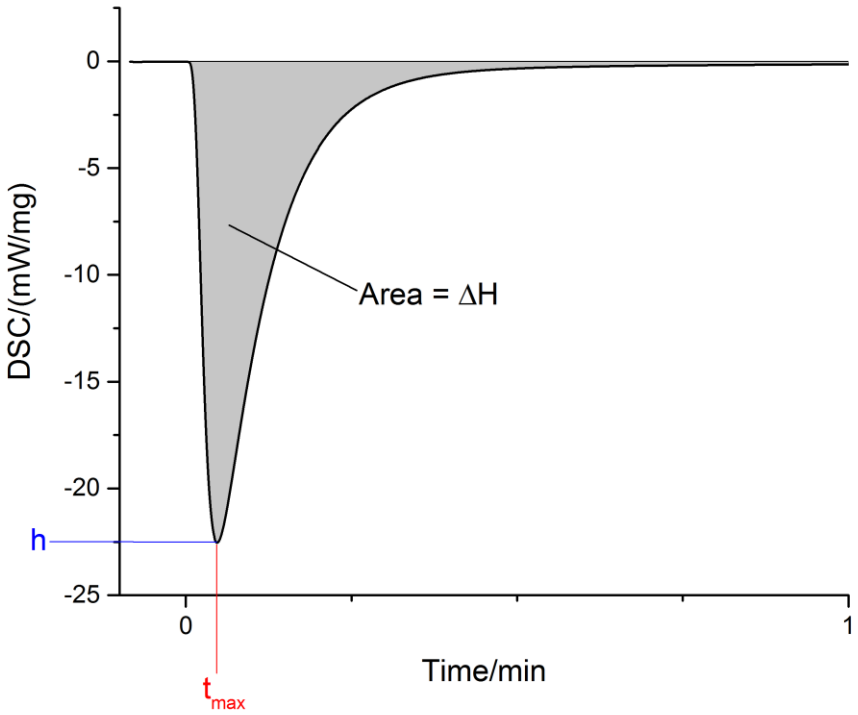

Figure 5 Analysis of a Photo-DSC curve.

With the Photo-DSC, various parameters can be obtained by using only one single measurement. The reaction time (t_{max}) is the time to reach the maximum heat of polymerization. Additionally, the maximum heat flow can be determined by the peak height. Both, t_{max} and the peak height, reveal information about the curing speed of the resin. A flattened curve indicates a higher amount of time needed for the monomer conversion.

The overall reaction enthalpy H (peak area) is proportional to the conversion of the monomers in the curable system.

3. Results and Discussion

3.1. Preparation of the resin

During this work, a ternary system was investigated concerning its stability, reactivity and mechanical properties in the cured state. The basic composition of the resin consists of a multifunctional methacrylate, a tetrafunctional thiol and a difunctional alkyne.
The basic composition stated in Table 1 showed good results in previous workgroups of intern research and was, therefore, used.

Table 1 Molar ratio of the basic ternary system.

Difunctional methacrylate [mol]	**Tetrafunctional thiol [mol]**	**Difunctional alkyne [mol]**
4	1	1

Furthermore, a variable amount of different photoinitiators and stabilizers were added to the resin to investigate their influence on storage stability and photo reactivity.

3.1.1. Selection of the monomers

In a first step, an extensive search for suitable methacrylates was performed. For the ternary system the methacrylates should obtain crucial properties such as bifunctionality, a low viscosity and a rigid backbone to obtain good mechanical properties in the cured state. The following methacrylates showed interesting structures and were further investigated.

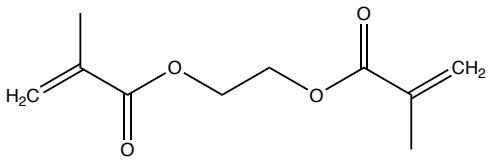

Ethylenglycol dimethacrylate (EGDMA)

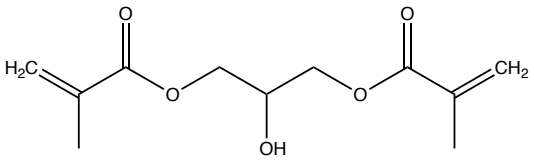

Glycerol dimethacrylate (GDMA)

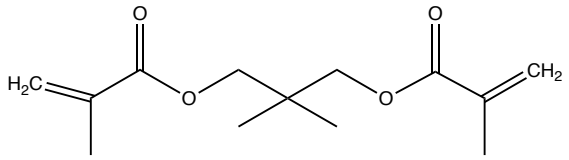

Neopentylglycol dimethacrylate (NPGDMA)

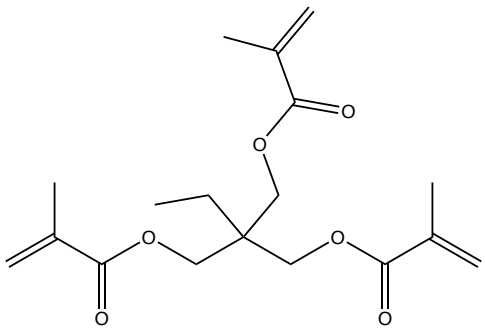

Trimethylolpropan trimethacrylate (TMPTMA)

Scheme 5 Used methacrylates.

Glycerol dimethacrylate (GDMA) possesses a free, polar OH-group which is expected to improve the dispersibility of the filler material. Neopentylglycol dimethacrylate (NPGDMA) was chosen because of its rigid backbone and increases in thermo mechanical properties were assumed. Ethylenglycol dimethacrylate (EGDMA) was chosen because of its usage for dental filling materials and its agreeable biocompatibility.[57] Apart from the bifunctional methacrylates, the trifunctional methacrylate trimethylolpropan trimethacrylate (TMPTMA) was investigated. For the trifunctional methacrylate, a faster curing rate due to an accelerate network formation was expected. Also, a low methacrylate migration was assumed based on the increase of reactive centers. TMPTMA was mainly studied to enhance the reactivity in methacrylate blends.

As a tetrafunctional thiol the commercially available Pentaerythitol tetra(3-mercaptopropionat) (PETMP) (see Scheme 6) was investigated.

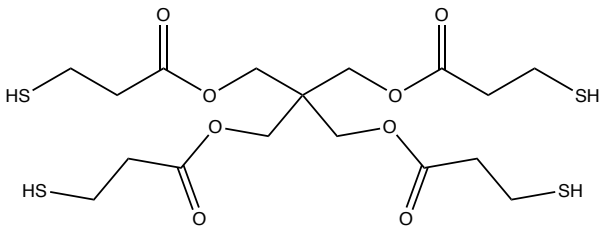

PETMP

Scheme 6 Used thiol.

For the third component of the ternary system the two alkynes (Scheme 7) di(but-3-yn-1-yl) carbonate (DBC) and di(prop-2-yn-1-yl) carbonate (DPC) were used.

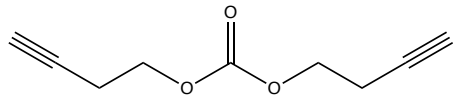

DBC

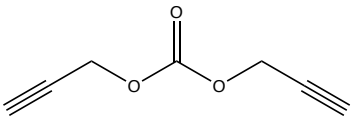

DPC

Scheme 7 Used alkynes.

These alkyne carbonates were obtained in a KOH-catalyzed single-step reaction. Both synthesis were carried out with 1,1'-carbonyldiimidazole (CDI) and an excess of either 3-butyn-1-ol (for DBC) or 2-propyn-1-ol (for DPC) suspended in toluene. After distillation, both products were obtained in good yields. (89-91%)

3.1.2. Selection of the stabilizers

One of the main purposes of this thesis was to obtain a stable ternary formulation. Therefore, different stabilizers were examined.

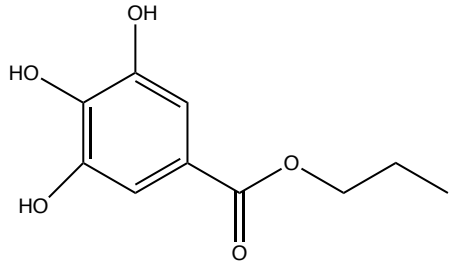

Propyl gallate

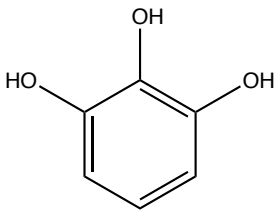

Pyrogallol

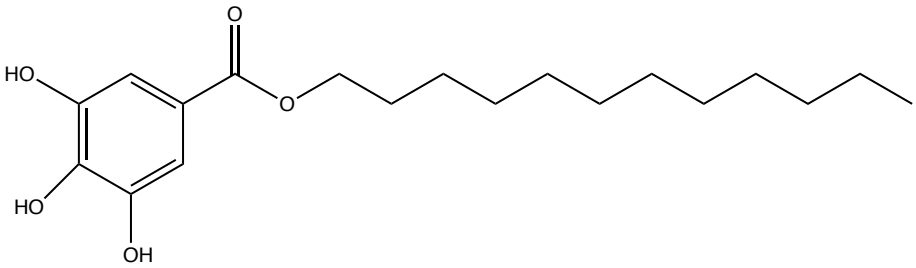

Lauryl gallate

Scheme 8 Used stabilizers.

Although the polymerization of ternary system is initiated by UV irradiation, non-UV indicated reactions can occur as well. This includes the spontaneous formation of radicals or the basic induced Thiol-Michael addition.[37] Therefore, radical scavengers and acidic stabilizers are crucial additives for the system.

Lauryl gallate and propyl gallate are both used as anti-oxidants in the food industry and both stabilizers are non-hazardous to health, which is very important for the usage of medical composite materials.[58] Furthermore, previous workgroup intern research showed that propyl gallate, as well as pyrogallol, are an excellent stabilizer in thiol-yne systems.[39]

However, there are concerns about the toxicity of pyrogallol as it is not suitable for biocompatible resins. However, it can be applied to binder materials for ceramic particles. These binder materials are sintered after the printing process which causes the removal of all organic substances leaving only a pure ceramic specimen behind.

For the prevention of the basic induced Thiol-Michael-Addition Miramer A99 (Scheme 9) was used. It consists of a phosphoric ester with either an hydrogen or a methacrylate as a substituent.

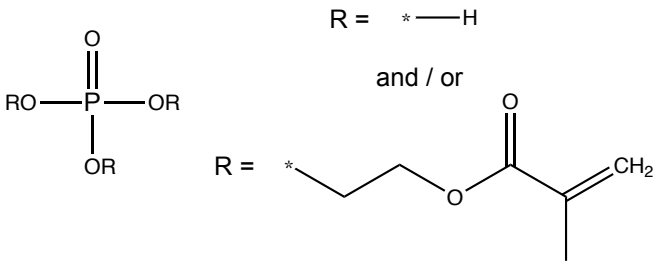

Scheme 9 Miramer A99.

The methacrylate group in Miramer A99 is able to polymerize into the network. It is expected to have a positive influence on the migration behavior of this stabilizer.

Liska et al. reported a promising heterosynergistic system consisting of an acidic stabilizer combined with a radical scavenger.[40] Previous group-intern research showed good results for Miramer A99 as an acidic stabilizer. Therefore, Miramer A99 was applied combined with different anti-oxidant stabilizers in all resin formulations.

3.1.3. Selection of the photoinitiators

For UV curable systems and especially 3D printable formulations, a fast curing rate is crucial. A longer curing rate leads to a slow printing process which makes the application of the resin economically unviable. For this reason, different photoinitiators (see Scheme 10) in different concentrations were evaluated.

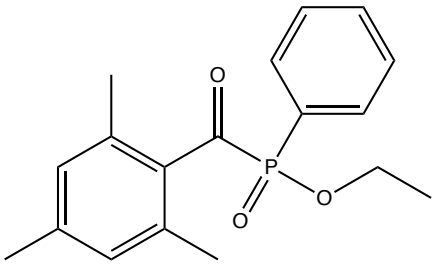

Irgacure TPO-L

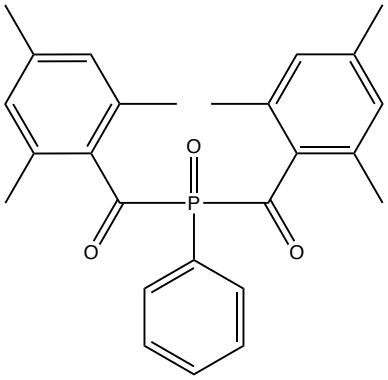

Irgacure 819 BAPO

Scheme 10 Used photoinitiators.

Both photoinitiators absorb in the long wavelength range near the visible region at 400 nm. Ethyl(2,4,6-trimethylbenzoyl)phenylphosphinate (TPO-L) is liquid which has the main advantage that it can be easily incorporated in formulations whereas bisacyl phosphine oxide (BAPO) comes as powder and needs to be dissolved.

3.2. Evaluation and improvement of the storage stability of ternary systems

For applications in the industrial sector, a long shelf-life of the resin is required. Therefore, the stabilizer system should prevent premature polymerization of the ternary system and avoid significant viscosity increase. Since a long term evaluation of the resin formulations at room temperature would be too time-consuming, the tests were carried out at increased temperature. According to Arrhenius, a temperature increase of 10 °C doubles the reaction rate.

A stabilizer system showing a low increase of viscosity over several days at increased temperature was the desired achievement. For the storage stability tests the samples were stored at a specific temperature over several days. Each stabilizer system consists of 4 mol% Miramer A99 and a variable amount of an anti-oxidant stabilizer. The ideal Miramer A99 concentration for ternary formulations was evaluated in workgroup intern research. The study showed a good stabilization for 4 mol% Miramer A99. Since a decline in mechanical properties for higher concentrations of Miramer A99 was assumed, 4 mol% were used for the stabilizer system. Therefore, this Miramer A99 concentration was maintained and not altered any further. The viscosity changes of the resin were documented regularly via a rheometer.

3.2.1. First evaluation of the storage stability

To get a quick overview of the working stabilizer systems, the first storage stability tests were performed with only one methacrylate. The following tests were carried out with PETMP as thiol, DPC as alkyne and GDMA as methacrylate. The samples were stored at 90°C to get quick results about which stabilizer works best. All storage stability tests were carried out in duplicate determination to reduce measurement uncertainties.
Table 2 states the evaluated stabilizer systems.

Table 2 Stabilizer system for the first storage stability test at 90 °C.

System	[mol %]	1st radical scavenger	[mol %]	2nd radical scavenger	[mol %]	Acid stabilizer
1	2	Propyl gallate	-	-	4	Miramer A99
2	3					
3	2	Propyl gallate	0.5	Lauryl gallate		
4	3					
5	4					
6	2	Propyl gallate	1	Lauryl gallate		
7	3					
8	4					
9	5					
10	1	Pyrogallol	-	-		
11	2					
12	3					

In Figure 6 all results are summarized.

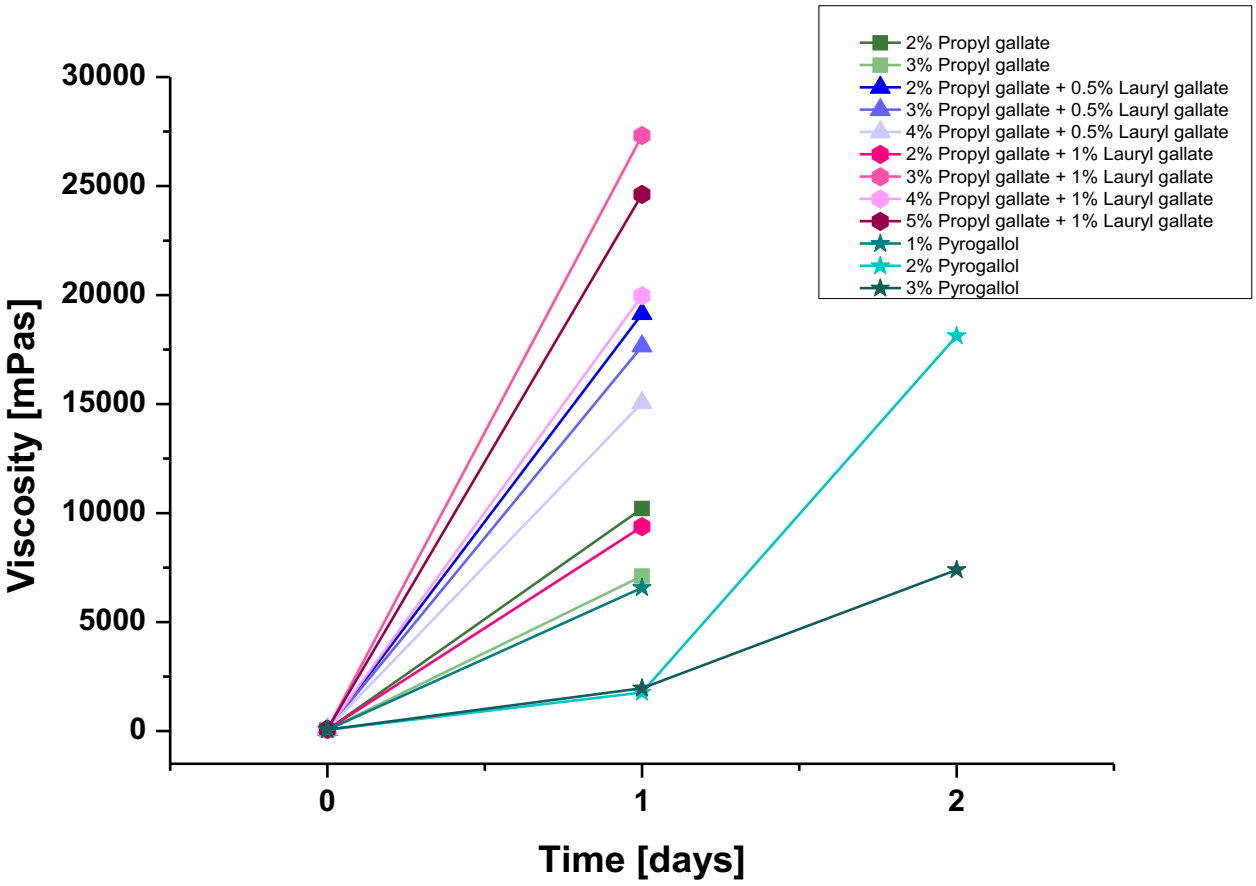

Figure 6 Storage stability of a ternary system consisting of PETMP, DPC and GDMA at 90 °C. Termination of the lines indicate the day of solidification.

The obtained results show that most of the samples were completely cured after two days. Even though group intern research investigated a good stabilization of thiol-yne system with propyl gallat, the ternary system could not be stabilized. This is mainly due to the challenging stabilization of the thiol-ene reaction between the thiol and the methacrylate.[39,40]

Furthermore, the combination of propyl gallate and lauryl gallate was also not able to improve the storage stability.

Only pyrogallol showed promising results since the resins with 2% and 3% pyrogallol were measurable after two days.

To obtain a test series over a longer period of time the analysis was repeated at 50 °C storage temperature. A temperature of 50 °C provides a temperature high enough to accelerate the reaction rate of the resins. Moreover, the temperature is low enough to extend the observation time to gain more detailed information about the efficiency of the stabilizer.

For the storage stability test series at 50°C, the following stabilizer systems stated in Table 3 were evaluated.

Table 3 Stabilizer systems for a storage stability test at 50°C.

System	[mol %]	1st radical scavenger	[mol %]	2nd radical scavenger	[mol %]	Acid stabilizer
13	2	Propyl gallate	-	-	4	Miramer A99
14	3					
15	4					
16	5.5					
17	2	Propyl gallate	0.5	Lauryl gallate		
18	4					
19	2	Propyl gallate	1	Lauryl gallate		
20	4					
21	2	Pyrogallol	-	-		
22	3					
23	4					

The results for the storage stability test at 50 °C are depicted in Figure 7.

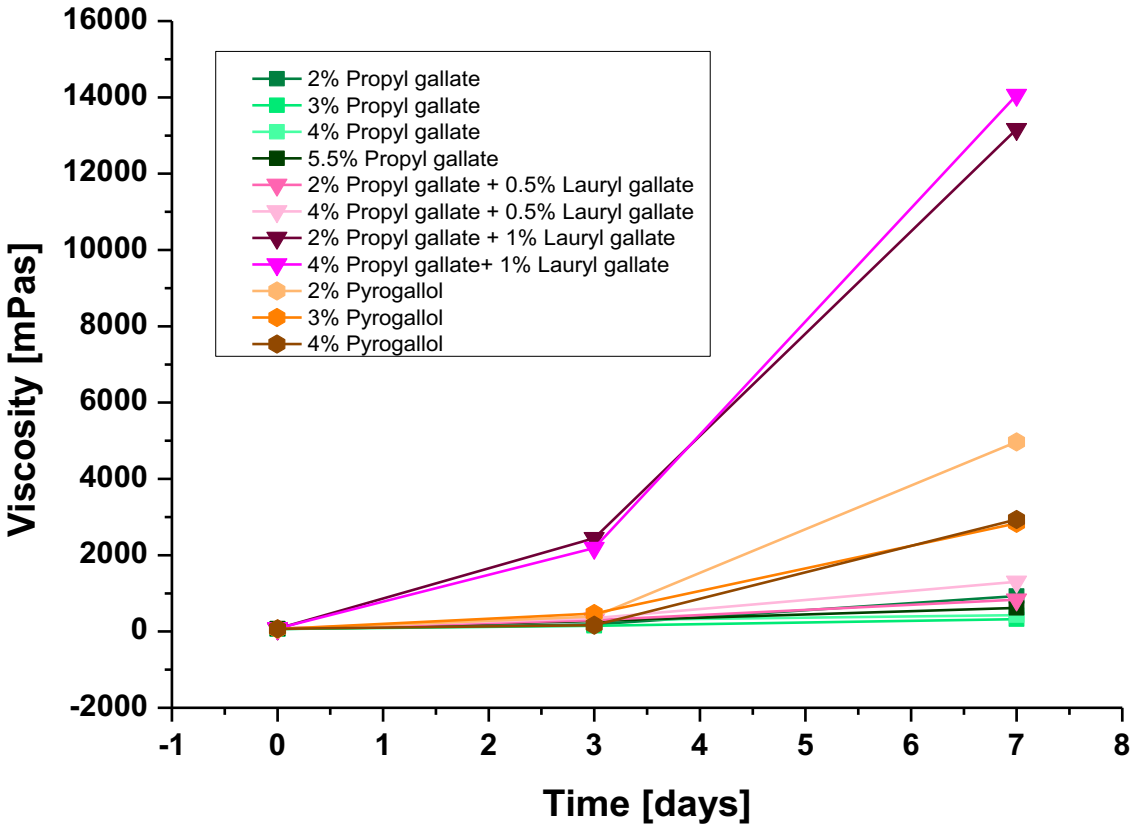

Figure 7 Storage stability of a ternary system with PETMP, DPC and GDMA at 50 °C.

A longer observation period of the several ternary systems was given at 50°C. Compared to 90 °C the propyl gallate showed quite promising results and surpassed even pyrogallol. This unexpected result needed further investigation and, therefore, the impact of propyl gallate and pyrogallol were studied with each methacrylate.

Even though the system with propyl gallate and 0.5% lauryl gallate showed good results, lauryl gallate was not considered any longer because of its bad solubility. It was not possible to obtain a homogeneous solution with higher concentrations than 0.5% of lauryl gallate.

As a result, ternary systems with each tested methacrylate were evaluated with different content of propyl gallate and pyrogallol.

3.2.2. Storage stability of all tested methacrylates

Since propyl gallate and pyrogallol showed the best results, the following storage stability tests for all tested methacrylates were carried out with these stabilizers. To each ternary system, 4 mol% Miramer A99 and either 4 mol% propyl gallate or 4 mol% pyrogallol were

added. The samples were stored at 50 °C for several days and the results are summarized in Figure 8.

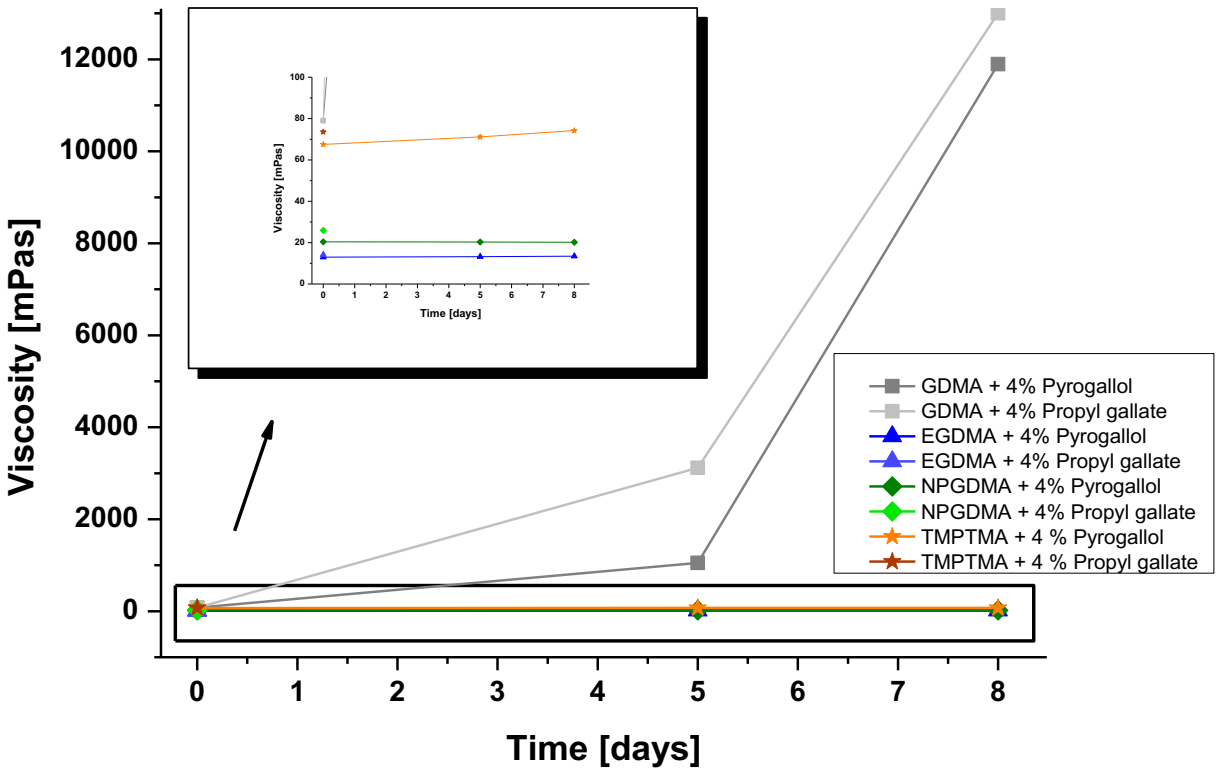

Figure 8 Storage stability of a ternary system with PETMP, DPC and different methacrylates with 4% propyl gallate or pyrogallol. Termination of the lines indicate the day of solidification.

It can be seen that no ternary system, except the one with GDMA, was managed to be stabilized with propyl gallate. Nevertheless, the resin with GDMA showed the highest viscosity increase of all evaluated ternary systems. This ternary system, stabilized with pyrogallol, exhibited an increase of about 15000% within 8 days.

In contrast to this result, the stabilization of the ternary systems including TMPTMA, NPGDMA or EGDMA with pyrogallol showed nearly no viscosity increase. The high efficiency of pyrogallol as a radical scavenger in thiol-ene systems has already been reported.[39] This enhanced performance is mainly due to the resonance stabilization of the formed pyrogallol radical.

Since GDMA showed the least promising storage stability of all methacrylates, it was not further considered for the final ternary system.

Figure 9 displays the viscosity increase of 4 mol% pyrogallol and 4 mol% Miramer A99 in more detail.

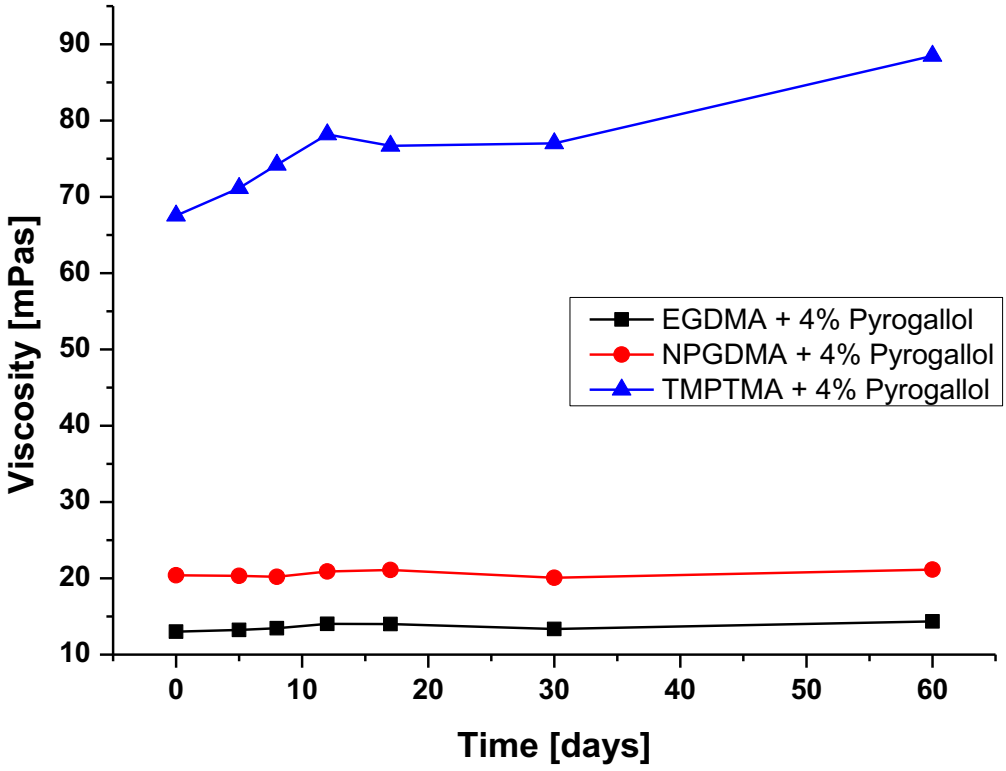

Figure 9 Stabilization of the ternary system with 4% pyrogallol and 4% Miramer A99.

The ternary system containing TMPTMA as methacrylate showed a significant higher start viscosity compared to EGDMA and NPGDMA. Even after 60 days the viscosity increase of the ternary system with TMPTMA did not exceed 31%. Additionally, no viscosity increase regarding the systems with EDGMA and NPGDMA was detected. Based on these results, further investigations were carried out with 4 mol% pyrogallol

3.3. Investigation of the photoreactivity of ternary systems

For 3D printing the curing time of the resin plays an important role and, therefore, a fast curing rate is desired. For the determination of the photoreactivity and monomer conversion of the ternary systems with different methacrylates Photo-DSC was used.

Photo-DSC allows to obtain a variety of parameters with only one single measurement. For instance, t_{max} refers to the time needed to reach the maximum heat of polymerization. The height of the peak refers to the maximum heat flow during the reaction and the overall

reaction enthalpy is proportional to the monomer conversion. For the ideal dimethacrylate of the ternary system, a fast curing and a high monomer conversion is requested. This means that a low t_{max}, a high peak and a high ΔH are crucial for the system.
According to these measurements the most suitable methacrylate for the final ternary resin was evaluated. Subsequently, further investigations on the impact of the stabiliziers and on the photoinitiators were conducted.

3.3.1. Overview

The following Table 4 represents the formulation of the ternary system for the first reactivity screening via Photo-DSC. All ternary systems were tested on the influence of different stabilizer systems and their impact on the photoreactivity. For reference values the systems were also investigated without any stabilization at all.

Table 4 Composition of the ternary system for the first reactivity screening.

System	Thiol	Alkyne	Meth-acrylate	Radical scavenger	Acid stabilizer	Photo-initiator
1	PETMP	DPC	GDMA	4 mol% pyrogallol	4 mol% Miramer A 99	0.5 wt% TPO-L
2				4 mol% propyl gallate		
3				Without stabilizer system		
4	PETMP	DPC	EGDMA	4 mol% pyrogallol	4 mol% Miramer A 99	0.5 wt% TPO-L
5				4 mol% propyl gallate		
6				Without stabilizer system		
7	PETMP	DPC	NPGDMA	4 mol% pyrogallol	4 mol% Miramer A 99	0.5 wt% TPO-L
8				4 mol% propyl gallate		
9				Without stabilizer system		
10	PETMP	DPC	TMPTMA	4 mol% pyrogallol	4 mol% Miramer A 99	0.5 wt% TPO-L
11				4 mol% propyl gallate		
12				Without stabilizer system		

The following Figure 10-Figure 13 display the results of the photoreactivity for each ternary resin with different stabilizer systems.

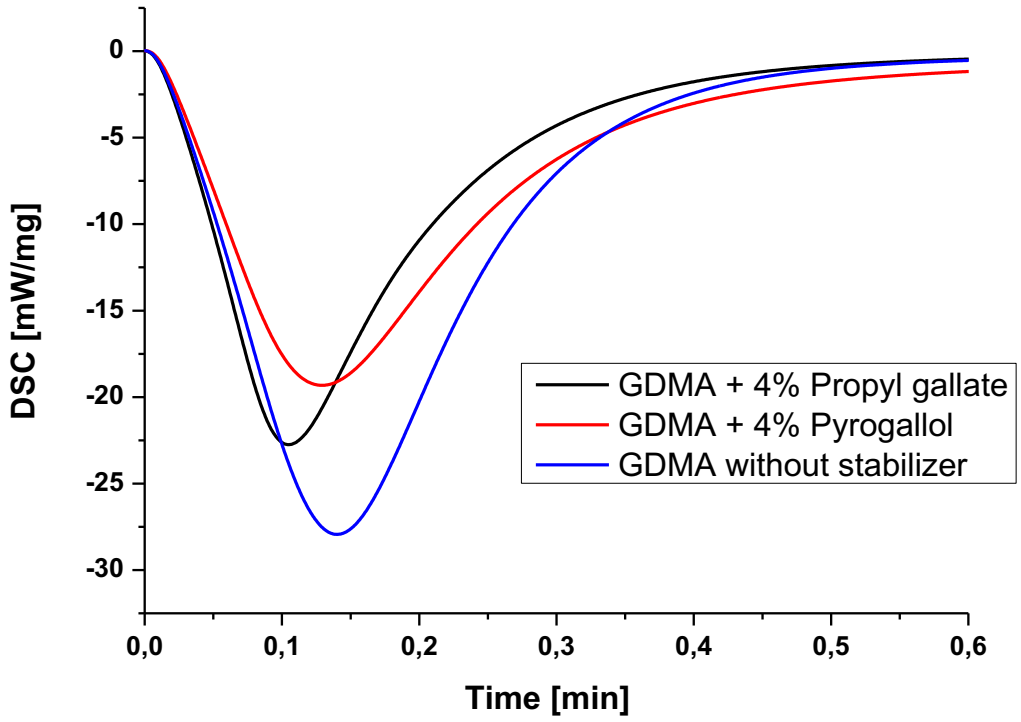

Figure 10 Photo-DSC measurement of a ternary system with PETMP, DPC and GDMA containing different stabilizers.

The results seen in Figure 10 are summarized in Table 5.

Table 5 Photo DSC results of a ternary system with PETMP, DPC and GDMA containing different stabilizers.

Composition	t_{max} [s]	Peak height [mW/mg]	ΔH [J/g]
GDMA + 4 % pyrogallol	7.3	19.8	311
GDMA + 4 % propyl gallate	7.9	21.6	317
GDMA without stabilization	8.3	27.9	350

The ternary system with GDMA displays a fast reaction rate which makes this methacrylate interesting for the application in 3D-printing processes. Also, this ternary system shows a sufficient monomer conversion. This leads to the assumption that the cured polymer consists of fewer unreacted monomers which can migrate.

The addition of a stabilizer system to the resin leads to a decrease in the peak height and ΔH. Although the system with pyrogallol shows the lowest t_{max} value, it exhibits a decrease by 40% in peak height and 12% in monomer conversion compared to the unstabilized system.

Since the storage stability of GDMA was not sufficient enough it was not further considered for the final ternary system. Therefore, the results of the reactivity of this methacrylate are not taken into account.

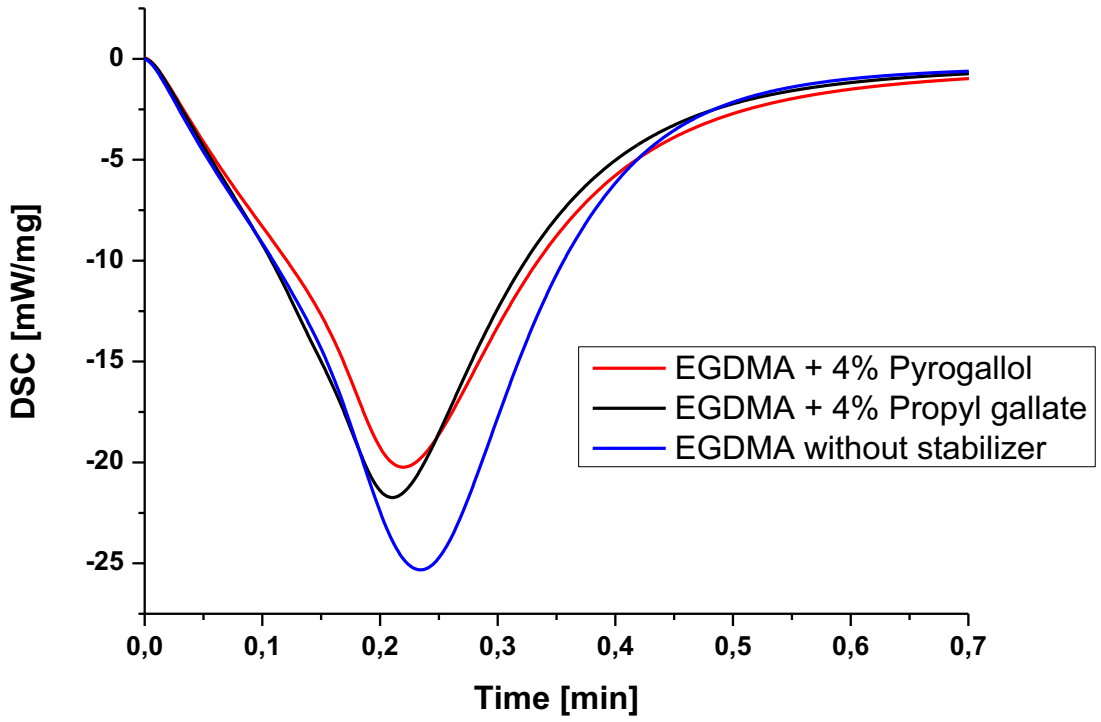

Figure 11 Photo-DSC measurement of a ternary system with PETMP, DPC and EGDMA containing different stabilizers.

The results seen in Figure 11 are summarized in Table 6.

Table 6 Photo DSC results of a ternary system with PETMP, DPC and EGDMA containing different stabilizers.

Composition	t_{max} [s]	Peak height [mW/mg]	ΔH [J/g]
EGDMA + 4% pyrogallol	13.1	20.2	341
EGDMA + 4% propyl gallate	12.7	21.7	320
EGDMA without stabilization	14.3	23.3	386

Compared to the other methacrylates, EGDMA shows an unsatisfying reaction rate. For 3D-printing applications a fast curing rate is required which makes this ternary system not applicable for AMT. A considerable benefit of this methacrylate is its high monomer conversion. Nevertheless, the slow reaction rate is a major drawback and, therefore, EGDMA is not considered for the final ternary system.

Moreover, an influence of the stabilizer system can be seen. Compared to the unstabilised system, the peak height decreases by about 15% and ΔH by 13%.

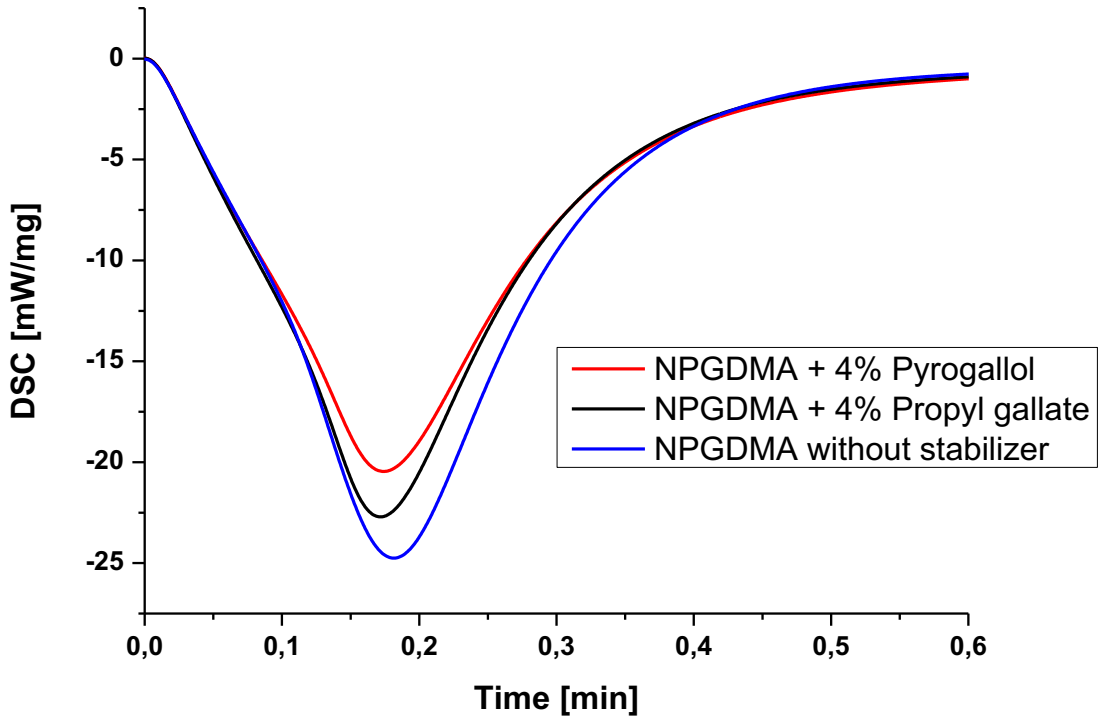

Figure 12 Photo-DSC measurement of a ternary system with PETMP, DPC and NPGDMA containing different stabilizers.

The results seen in Figure 12 are summarized in Table 7.

Table 7 Photo DSC results of a ternary system with PETMP, DPC and NPGDMA containing different stabilizers.

Composition	t_{max} [s]	Peak height [mW/mg]	ΔH [J/g]
NPGDMA + 4% pyrogallol	10.4	20.5	297
NPGDMA + 4% propyl gallate	10.3	22.7	295
NPGDMA without stabilization	10.7	24.8	331

The reaction rate for NPGDMA is average compared to the alternative methacrylates. Nevertheless, the rigid backbone structure of the molecule makes this methacrylate highly interesting for the ternary system.

Again, a decrease in the peak height and ΔH can be detected for the stabilized systems. The peak height decreases by around 21% and the monomer conversion exhibits a decrease by around 11%.

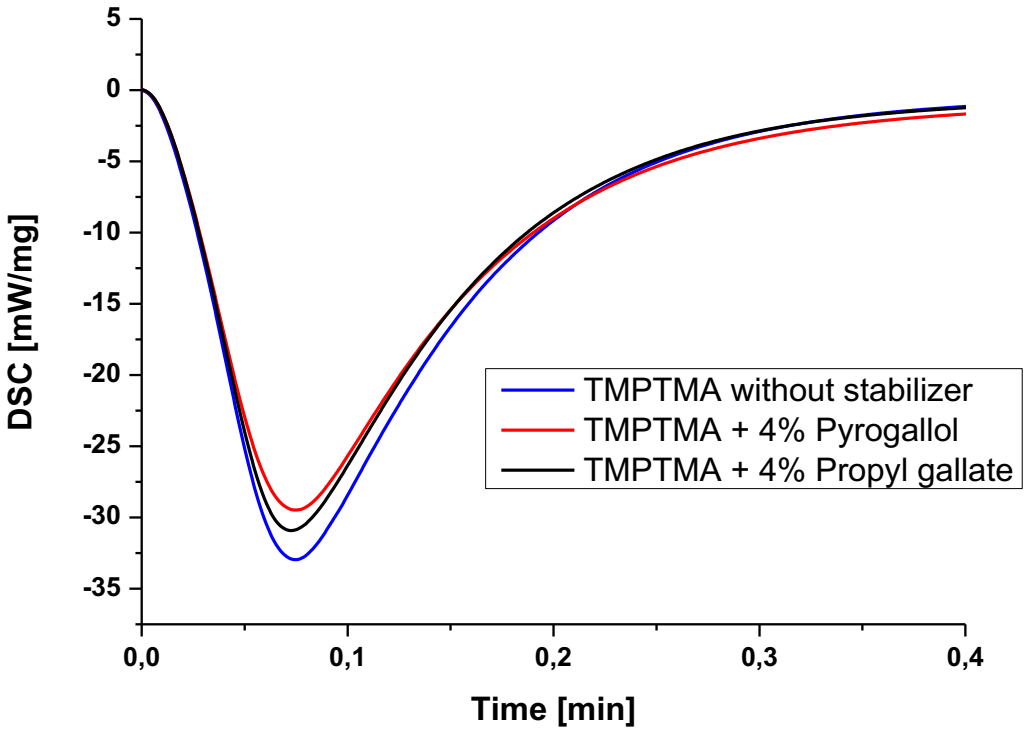

Figure 13 Photo-DSC measurement of a ternary system with PETMP, DPC and TMPTMA containing different stabilizers.

The results seen in Figure 13 are summarized in Table 8.

Table 8 Photo DSC results of a ternary system with PETMP, DPC and TMPTMA containing different stabilizers.

Composition	t_{max} [s]	Peak height [mW/mg]	ΔH [J/g]
TMPTMA + 4% pyrogallol	4.3	29.5	309
TMPTMA + 4% propyl gallate	4.3	30.9	287
TMPTMA without stabilizer	4.3	33.0	292

By far the highest reaction rate is shown by the trifunctional methacrylate TMPTMA, but it exhibits a low value for ΔH. Moreover, it can be assumed from the structure of the trifunctional methacrylate that the resulting polymer will obtain unwanted brittle properties. Furthermore, the network formation of the trifunctional methacrylate occurs at a higher rate and yields a higher network density compared to difunctional methacrylates. This can induce a higher shrinkage stress during curing which leads to brittle materials.

Unlike the other ternary systems, this resin shows the highest ΔH value for the stabilized system with pyrogallol. This could be explained by the high reactivity of this resin. The polymerization were initiated before the Photo-DSC measurement started which yields lower

values for the monomer conversion. Nevertheless, the stabilized system showed a decrease in the peak height of about 12%.

Summing up, a decrease concerning the photoreactivity could be detected for all stabilized resins.

3.3.2. Methacrylate blends

TMPTMA showed promising results concerning the curing speed and NPDGMA possesses sufficient monomer conversion. Additionally, NPDGMA consists of an interesting molecular structure which is assumed to feature good mechanical properties. For this reason, both methacrylates were blended to combine their best properties. In this way, it was investigated which ratio of the methacrylates would be the most suitable. Additionally, the impact of different photoinitiators was tested. These two investigations were carried out to obtain the highest possible reaction rate with the best monomer conversion. To the basic composition (Table 9) the methacrylates, TMPTMA and NPGDMA, are added in various concentrations.

Table 9 Basic composition of the methacrylate blends.

Thiol	Alkyne	Radical scavenger	Stabilizer	Photoinitiator
PETMP	DPC	4% pyrogallol	4% Miramer A 99	0.25% TPO-L + 1% BAPO
				0.5% TPO-L + 2% BAPO
				0.75% TPO-L + 3% BAPO

The Photo-DSC analysis (Figure 14) illustrates that the ternary system shows the highest photo-reactivity with a methacrylate composition of 30% TMPTMA and 70% NPGDMA compared to a system consisting of only TMPTMA as methacrylate.

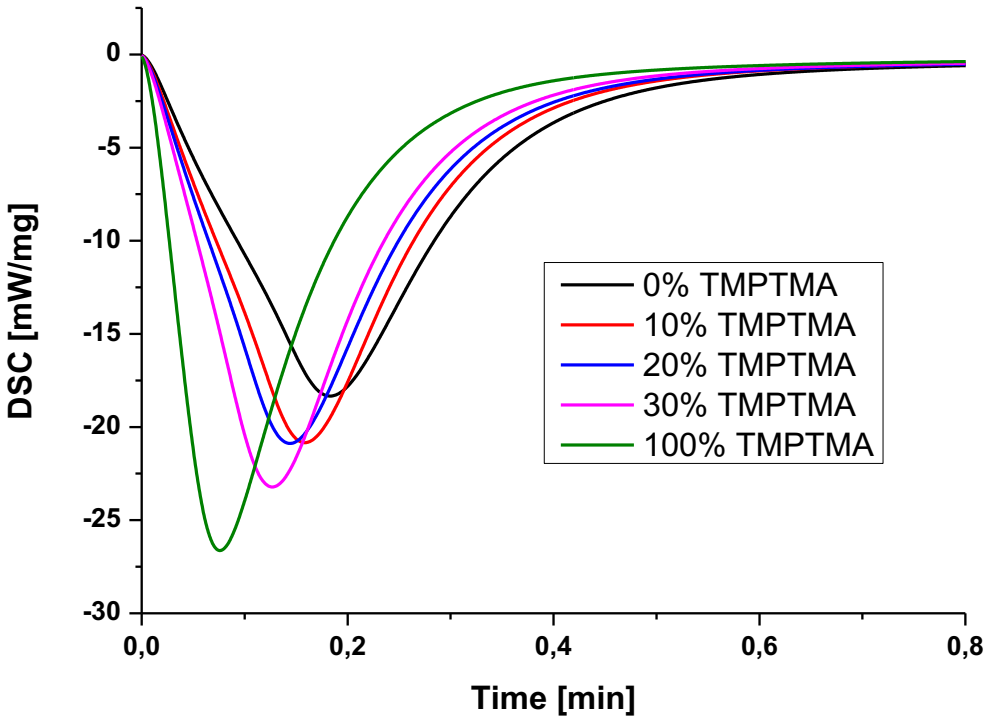

Figure 14 Photo-DSC measurement of methacrylate blends for the ternary system containing 2% BAPO and 0.5% TPO-L.

The influence on the reaction rate of the different methacrylate ratios are depicted in Figure 15 - Figure 16.

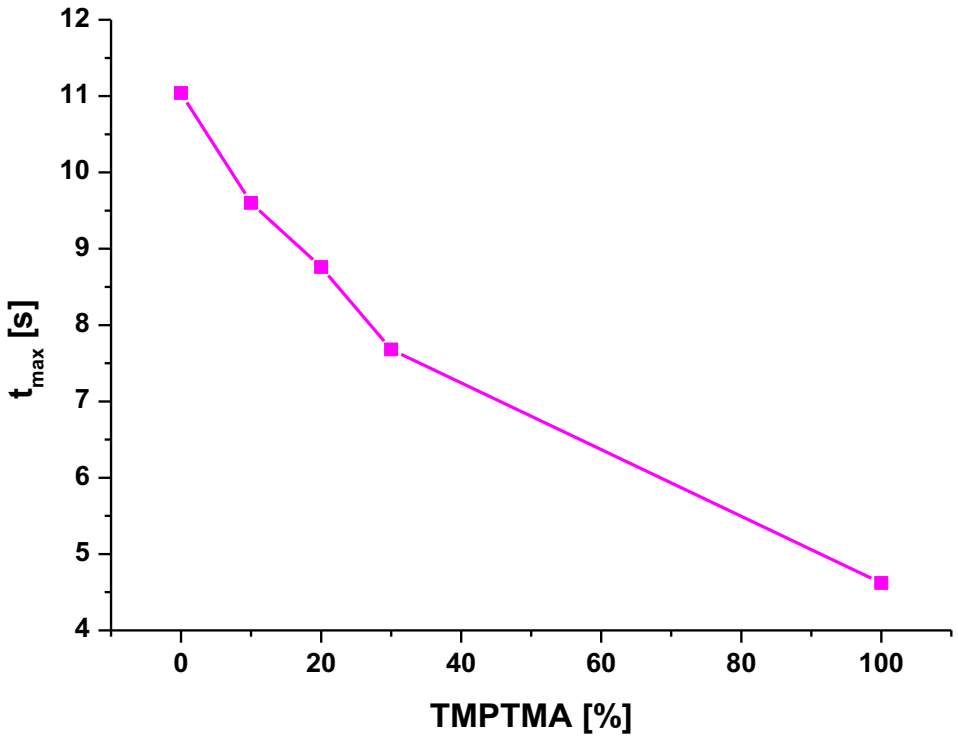

Figure 15 Influence on the reaction rate for increasing TMPTMA concentrations in a ternary system containing 2% BAPO and 0.5% TPO-L. The line is a guide for the eye.

With the addition of TMPTMA to NPDGMA the reaction rate increased significantly. The ternary system with only NPDGMA exhibited a rather slow curing rate. Such a long reaction time is a drawback for the application of the resin in AMT and, therefore, not suitable for the final ternary system. Nevertheless, a ratio of 30% TMPTMA and 70% NPDGMA leads to a decrease in t_{max} of about 44%. This significant increase in the curing rate makes the methacrylate blend interesting for 3D-printing processes.

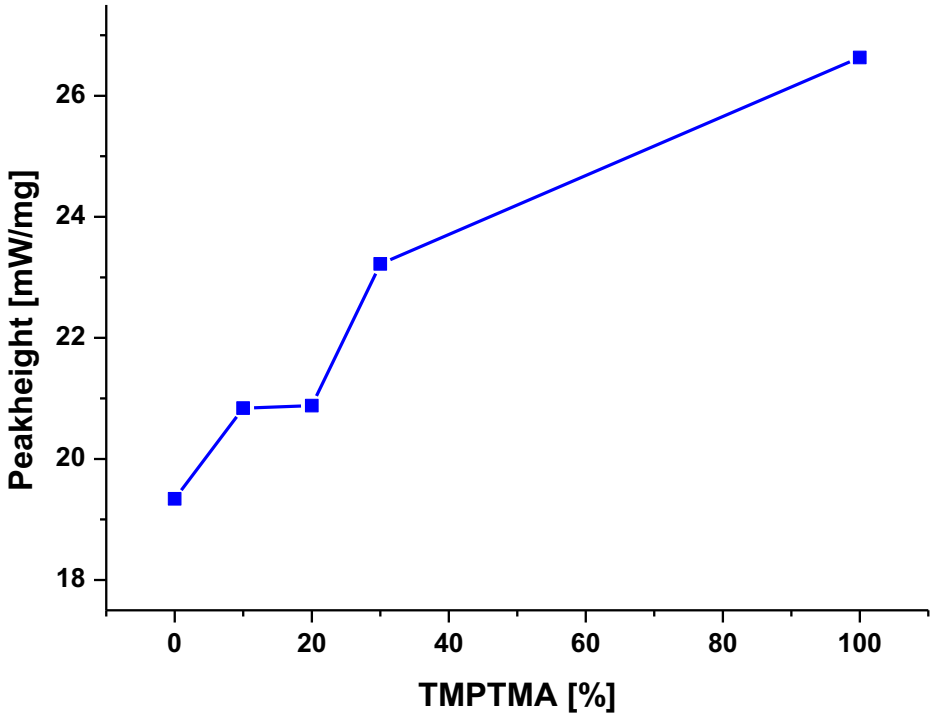

Figure 16 Influence on the Peakheight for increasing TMPTMA concentrations in a ternary system containing 2% BAPO and 0.5% TPO-L. The line is a guide for the eye.

Finally, the influence of the methacrylate blends on the peak-height was determined. Since the peak maxima are located in the negative x-axis, they refer to exothermic reactions. The highest peak is obtained by a ternary system consisting of only TMPTA as methacrylate. With the addition of a methacrylate blend of 30% TMPTMA and 70% NPGDMA the heat flow decreases by around 13%. Combined with the results of $t_{max,}$ a significant decrease in the reaction time could be obtained.

Also, an increase of around 4% in ΔH could be determined. Since ΔH is proportional to the monomer conversion, a high value is required.

This evaluation proofs that the best features of both methacrylates could be combined with a ratio of 30% TMPTMA and 70% NPGDMA.

Compared to a ternary system with only NPGDMA, the t_{max} could be reduced by 44%. In contrast to this, ΔH could be increased by 4% compared to ternary systems with only TMPTMA.

For further improvement of the photoreactivty different photoinitiator concentrations were also evaluated. The investigations were carried out with the same ternary system.

However, the major problem of the resin was the solubility of the BAPO photinitiator. 3% of this photoinitiator were nearly impossible to dissolve in the resin and, therefore, this concentration was not taken into account.

The Photo-DSC results of 1% BAPO and 1% TPO-L and 2% BAPO and 0.5% TPO-L for a 30% TMPTMA and 70% NPGDMA composition are summarized in Table 10.

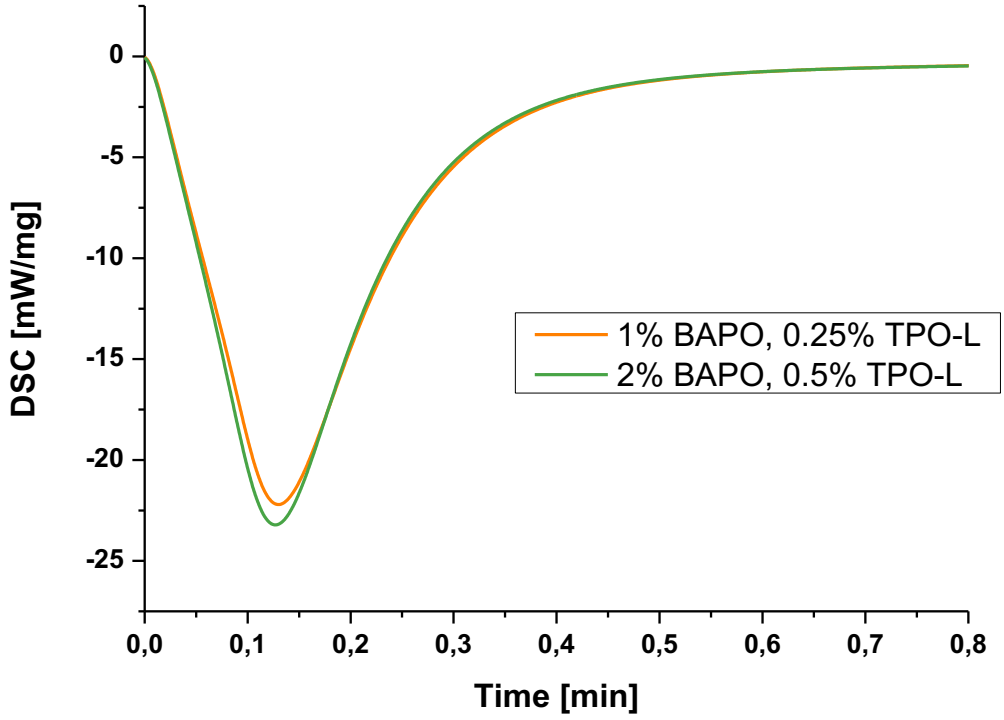

Figure 17 Photo-DSC measurement of a ternary system with different photoinitiators.

The results seen in Figure 17 are summarized in Table 10.

Table 10 Photo-DSC results for different photoinitiator concentrations.

Composition	t_{max} [s]	Peakheight [mW/mg]	ΔH [J/g]
1% BAPO + 0.25% TPO-L	7.8	22.2	298
2% BAPO + 0.5% TPO-L	7.7	23.2	300

For the final ternary system 2% BAPO and 0.5% TPO-L as photoinitiator system was chosen because it showed the highest number of reactivity and conversion. Furthermore, 2% BAPO can be easily dissolved in the resin.

3.3.3. Influence of the stabilizer on the photoreactivity

Finally, the influence of the pyrogallol concentration on the photoreactivity was studied. The aim of this investigation was a low concentration which provides a reactive system as well as a high storage stability. Therefore, the ternary system was tested with pyrogallol concentrations ranging from 1 to 4%. The composition of the resin can be seen at Table 11.

Table 11 Composition for the Photo-DSC evaluation of different stabilizer concentrations.

Thiol	Alkyne	Methacrylate	Stabilizer	Photoinitiator
PETMP	DPC	30% TMPTMA + 70% NPGDMA	Miramer A 99	0.5% TPO-L + 2% BAPO

Firstly, it was tested via Photo-DSC if higher stabilizer concentrations have an impact on the reactivity. The Photo-DSC curves can be seen in Figure 18.

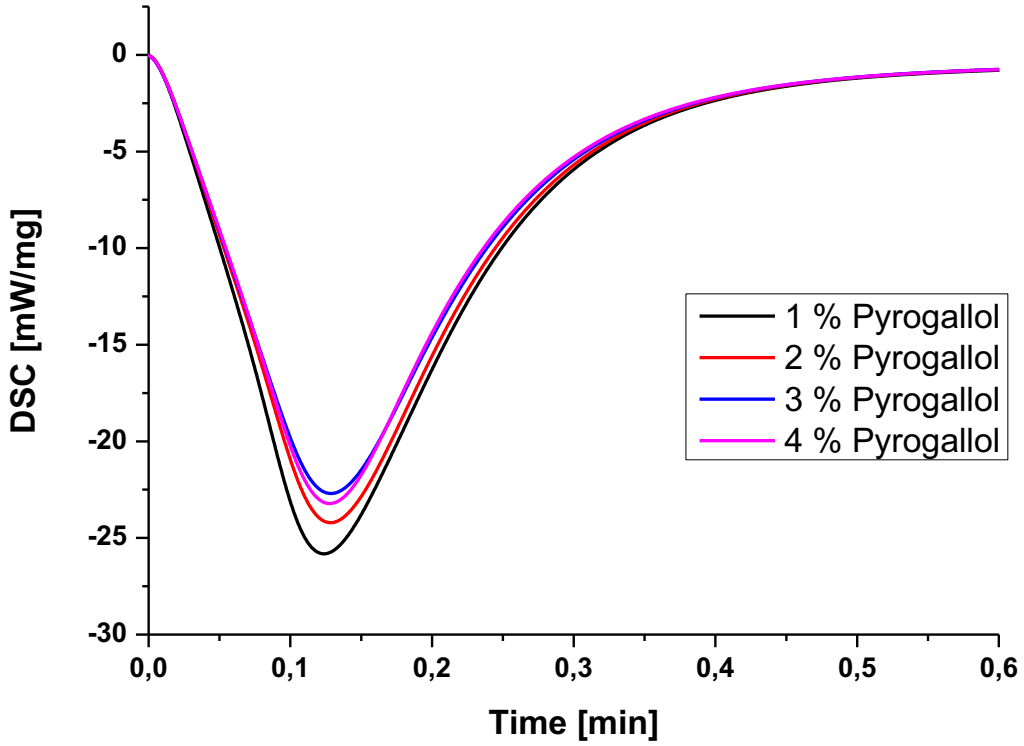

Figure 18 Photo-DSC measurement of the influence of varying pyrogallol concentrations on photo reactivity.

In Table 12 the results of the Photo-DSC are summarized.

Table 12 Results of the Photo-DSC evaluation of the influence of varying stabilizer concentrations on the photoreactivity.

System	t_{max} [s]	Peakheight [mW/mg]	ΔH [J/g]
1% Pyrogallol	7.6	25.9	343.3
2% Pyrogallol	7.9	24.2	322.9
3% Pyrogallol	7.9	22.7	305.9
4% Pyrogallol	7.9	22.0	291.8

The fastest reaction rate can be observed for 1% pyrogallol but the reaction rates among the higher concentrations only increased by around 4%. What can be seen very clearly is the decrease of the monomer conversion with increasing pyrogallol concentration. A decline in monomer conversion of about 18% can be depicted between 1% and 4% pyrogallol. A further disadvantage of high pyrogallol concentrations is the limited solubility of the stabilizer in the resin.

To find the most suitable concentration, a storage stability test at 50 °C for 1 and 2% pyrogallol was carried out. (see Figure 19)

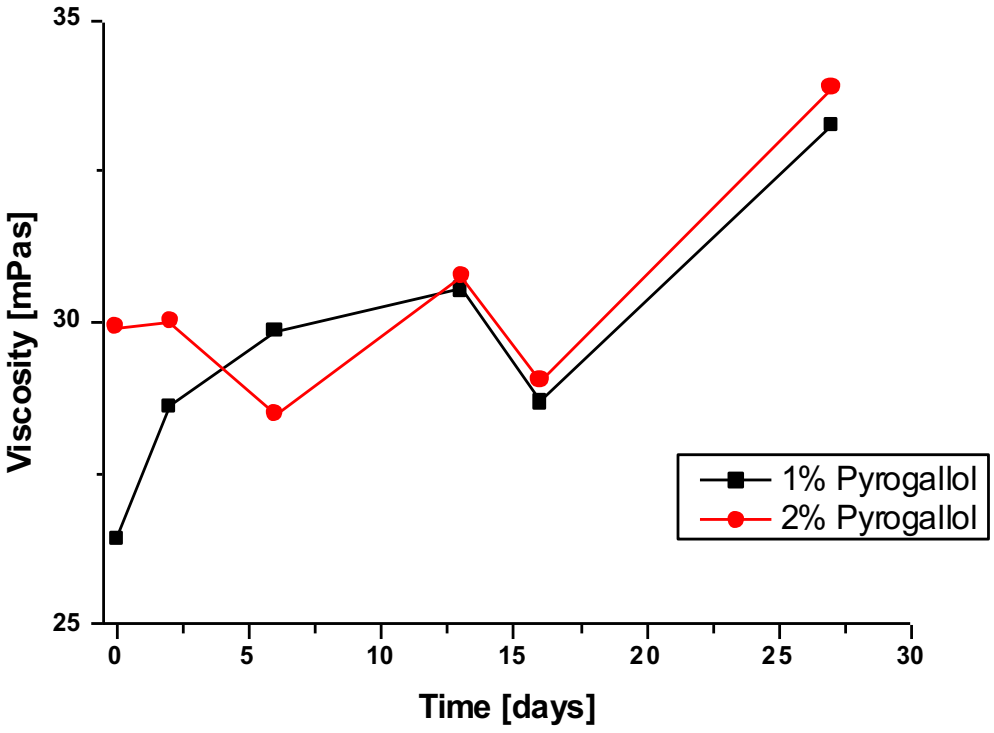

Figure 19 Storage stability test for different pyrogallol concentrations in methacrylate blends

The storage stability test showed no significant difference for 1 or 2% pyrogallol. Since 1% pyrogallol showed the fastest curing rate and the highest monomer conversion, this concentration was selected for the final monomer system.

3.4. Investigation of the monomer conversion via real time FT-IR analysis

Monomer conversion plays an important role regarding the biocompatibility. An incomplete monomer conversion can lead to subsequent migration of the remaining monomers out of the polymer. In the case of (meth)acrylates this can lead to high irritancy potential and cytotoxicity due to their function as Michael acceptor which can react with DNA molecules.[22–24]

Pure (meth)acrylate systems show comparably low conversion because these systems reach the gel point very early. The combination of methacrylate with a thiol/yne system can delay the gelation point, which has a positive influence on the monomer conversion.[30] Therefore,

a higher monomer conversion is expected for the ternary system compared to a pure methacrylate resin.

Furthermore, influence of different alkynes was studied as well. Previous research showed a high monomer conversion of thiol-yne system containing DBC as alkyne. Therefore, both carbonate alkynes, DPC and DBC, were compared.[27] The following systems stated in Table 13 were examined.

Table 13 Formulation of the ternary systems investigated in real time FT-IR analysis.

System	Thiol	Alkyne	Methacrylate	Radical scavenger	Stabilizer	Photoinitiator
1	PETMP	DPC	70% NPGDMA + 30% TMPTMA	1 mol% Pyrogallol	4 mol% Miramer A 99	0.5% TPO-L + 2% BAPO
2		DBC				

For the observation of the monomer conversion the liquid ternary system was placed between two CaF_2 platelets and 600 measurements were taken in series under the irradiation of light at 436 mW/cm^2 for 250 seconds.

To evaluate the reaction, the peaks of the alkyne C≡H stretch (~3280 cm^{-1}), the thiol S-H stretch (~2560 cm^{-1}) and the acrylate C=C stretch (~1640 cm^{-1}) were monitored. The integral area of the peaks during illumination was referenced to the initial value to show the consumption of the monomers and the reaction progress. The methacrylate conversions of the ternary systems with DBC or DPC and a pure methacrylate system are depicted in Figure 20.

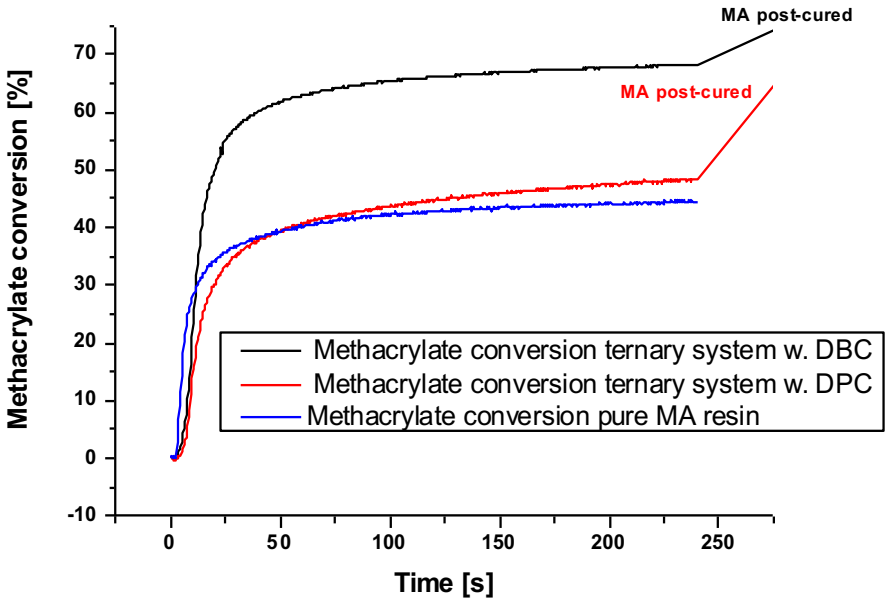

Figure 20 Methacrylate conversion in different resin systems.

As expected, the pure methacrylate system reached the lowest conversions with 40%. Furthermore, the ternary system with DPC showed lower conversion (45%) compared to the system with DBC (68%). All three systems were post-cured and measured again. For the post-curing the samples were heated to 100 °C for 10 minutes and treated with the lighthammer at 808 mW/cm^2 for one minute. The main purpose of the post-curing was to illuminate the cured samples above their T_g. This reactivated the mobility of the monomers and lead to a further polymerization of the unreacted functional moieties. The result of the post-curing was, therefore, an increase of the monomer conversion.

The post-curing had no influence on the pure methacrylate system and no further monomer conversion were achieved. The methacrylate conversion of the DPC system increased from 45% to 64% and the DBC system increased from 68% to 78%. The alkyne showed a big influence on the monomer conversion. Systems with DBC depicted a higher conversion compared to the systems with DPC.

The following Figure 21 shows the monomer conversion for all parts of the ternary system with DBC as alkyne.

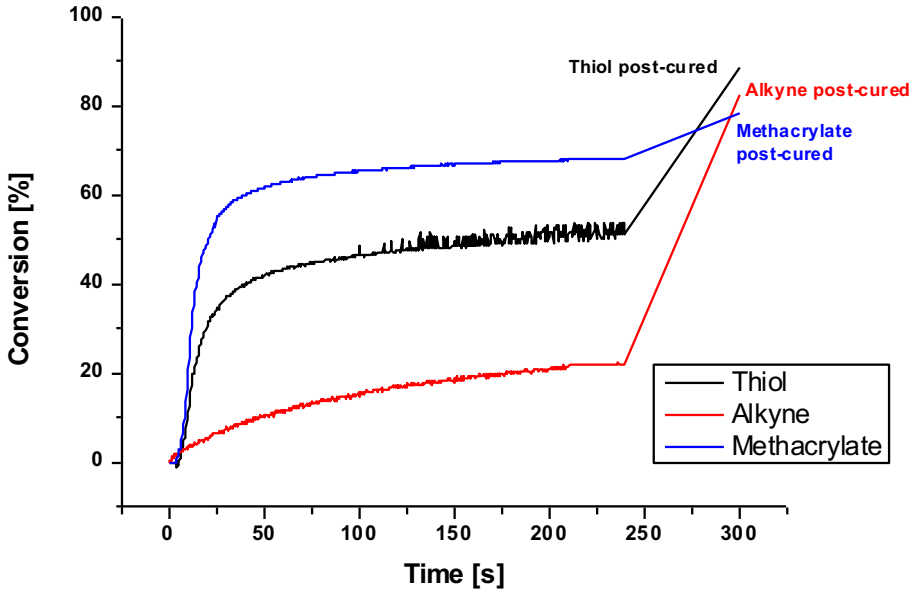

Figure 21 FT-IR analysis of all components of the ternary system with DBC.

The highest conversion can be obtained from the methacrylate (68%). This might be caused by the homopolymerization of the methacrylate and it can react with the thiol in a thiol-ene reaction. Lower conversion rates were investigated for thiol (45%) and the alkyne (20%). This can be explained with the faster proceeding of the thiol-ene reaction with the methacrylate. Since the methacrylate is more abundant than the alkyne, the probability of a thiol reaction with a C-C double bond is higher. Additionally, homopolymerization of the DBC is not possible. After post-curing, the conversion for the thiol and alkyne increased significantly. This lead to the assumption that the slower thiol-yne reaction took place during the post-curing process. The amount of converted thiol increased from 45% to 88%, alkyne from 20% to 82% and the methacrylate from 68% to 78%.

Even though a conversion of 100% was not obtained, there is a high probability that the vast majority of the monomers was firmly incorporated into the polymer matrix. This is due to the fact that all monomers are multifunctional and although not all functional groups reacted, there is a high chance that at least one moiety reacted and anchored the molecule in the matrix.

3.5. Migration analysis of cured ternary systems

To ensure that no hazard to health exists, a migration analysis of the cured system was carried out. Migration of methacrylates can be dangerous since a Thiol-Michael addition to the DNA is possible.[59]

For the analysis, the calibration standards of the to be examined molecules DPC, DBC, NPGDMA and TMPTMA in ethanol were provided at first. The curves are depicted in Figure 22 - Figure 25.

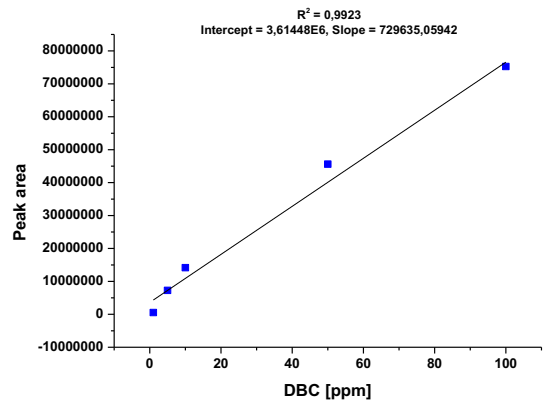

Figure 22 Calibration curve for migration analysis of DBC.

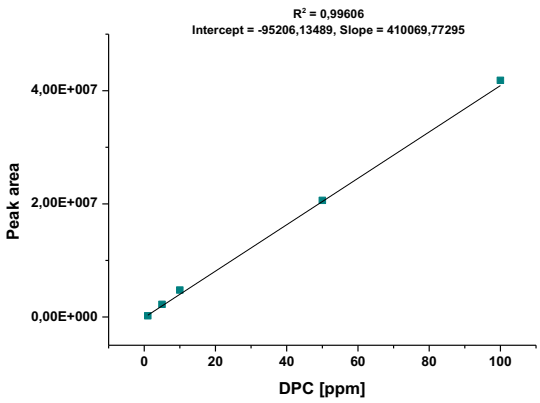

Figure 23 Calibration curve for migration analysis of DPC.

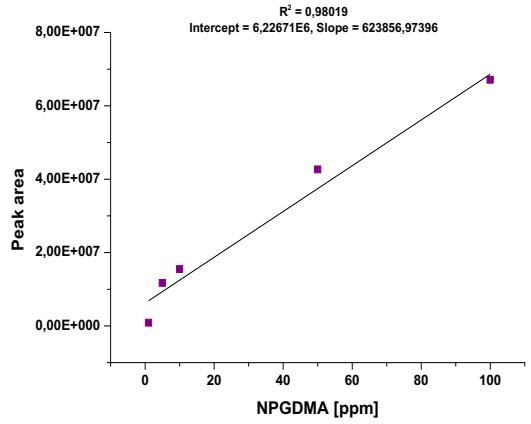

Figure 24 Calibration curve for migration analysis of NPGDMA.

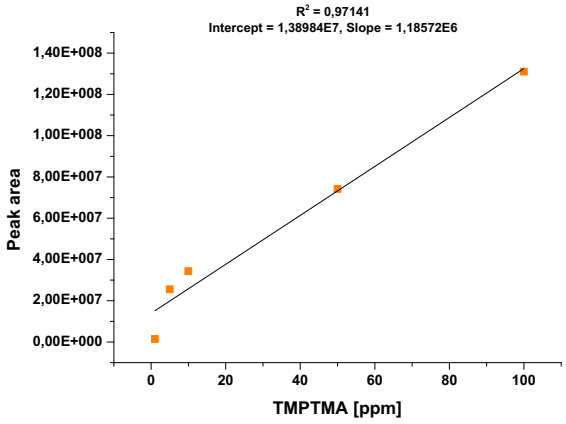

Figure 25 Calibration curve for migration analysis of TMPTMA.

Afterwards, 50 mg samples of both ternary systems with the same composition as for real time FT-IR analysis (Table 13) were cured via photo-DSC to obtain a fully cured polymer. The cured samples were stored in 1 ml of ethanol for one week at 50 °C and subsequently measured via GC-MS. The obtained peaks of the samples were compared to the calibration

standards of each molecule. In the following Table 14 the results of the GC-MS analysis are displayed.

Table 14 Results of the migration analysis of the ternary systems.

Formulation	DBC	DPC	NPGDMA	TMPTMA
DPC	-	0.33%	<detection limit	<detection limit
DBC	0.3%	-	<detection limit	<detection limit

Only for the alkynes a low migration could be detected. All other molecules migrated in such low concentrations that they did not even exceed the detection limit. Although the real time FT-IR analysis showed a conversion below 100%, the monomers were incorporated into the matrix so well that nearly no migration took place.

The obtained results show that the developed ternary system provides a promising performance concerning its application to the human body. Nevertheless, a migration analysis for the stabilizers pyrogallol and Miramer A99 needs to be done in upcoming projects.

3.6. Charpy impact test and heat deflection temperature of the ternary system

For the application in medical devices, such as implants, the polymer should be capable of absorbing a certain amount of energy. According to DIN EN ISO 179-, the charpy impact test can evaluate the amount of energy absorbed by a material during fracture. Also, the material should not deform in the body and thus a T_g above the maximum body heat (42 °C) is required. With the heat deflection temperature (HDT) measurement the temperature at which the polymer sample deforms under a specific load according to DIN EN ISO 75 can be determined. For both investigations polymer rods were needed which were cut out from a polymer plate. The polymer plates were produced with the ternary formulations stated in Table 15 containing either DBC or DPC and with a pure methacrylate formulation as reference.

Table 15 Formulations of the ternary and pure methacrylate systems used for the production of polymer plates.

System	Thiol	Alkyne	Methacrylate	Radical scavenger	Stabilizer	Photoinitiator
1	PETMP	DPC	70% NPGDMA + 30% TMPTMA	1 mol% Pyrogallol	4 mol% Miramer A 99	0.5% TPO-L + 2% BAPO
2		DBC				
3	-					

The plates were cured with the lighthammer at 55 mW/cm^2 and 323 mW/cm^2 for two minutes each and subsequently post-cured at 808 mW/cm^2 for one minute.

Apparently, the pure methacrylate system exhibited brittle properties and a high shrinkage stress. This effect was observed during the curing of the plates. Within a short amount of illumination time, the methacrylate plate started to rip which can be attributed to the experienced shrinkage stress as seen in Figure 26. It was not possible to obtain a usable plate for further tests. In comparison to this, the plates of the ternary system were obtained intact. This would be conform with previous investigations. It was evaluated that the addition of a thiol-yne system to a methacrylate delays the gel point resulting in a lower shrinkage stress.[31]

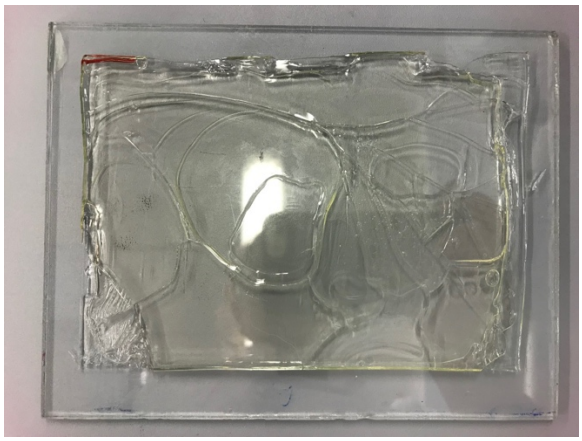

Figure 26 Pure methacrylate plate for charpy impact and HDT measurements after curing.

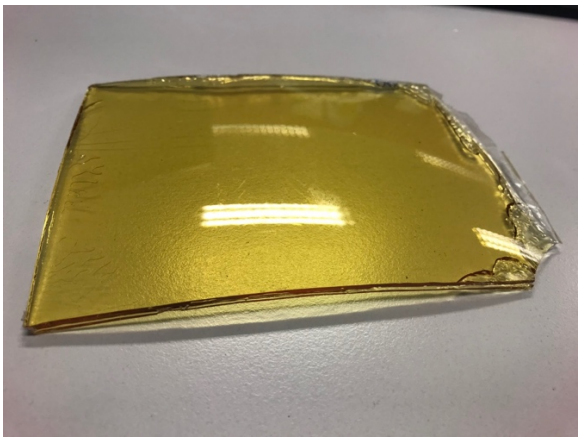

Figure 27 Plate of the ternary system with DPC for charpy impact and HDT measurements after postcuring.

During the post-curing process the DPC containing plate also experienced shrinkage stress. The plate bent sidewards as seen in Figure 26, making it difficult to cut proper rods out of it.

Still, it was possible to determine the impact strength and HDT for the DBC and DPC plate. The obtained results are depicted in Table 16.

Table 16 Results for the charpy impact test and HDT measurement.

System	Impact strength [kJ/m^2]	HDT [°C]
DBC	5 ± 0.25	171.3
DPC	2 ± 0.5	117.2

The impact strength values for both ternary systems indicate a brittle material. DPC shows far lower values compared to DBC, which could be explicable with a high shrinkage stress during post-curing. The higher shrinkage stress of the DPC system is explicable with the tighter network and its higher network density which results in brittle properties. Since the cracked methacrylate plate could not be measured, an improvement concerning brittleness and shrinkage stress in the ternary systems can only be assumed. The value of the HDT is referring to the temperature at which a material starts to deform. According to literature the pure methacrylate resins of poly(NPDGMA) and poly(TMPTMA) show both a T_g of 110 °C.[60,61] The addition of the thiol-yne system to the methacrylates lead to an increased T_g for the ternary system.

3.7. 3D printing of medical devices

For the 3D printing the curing time is crucial. Pure methacrylate systems exhibit a fast curing rate due to their rapid chain growth. In contrast, thiol-ene or thiol-yne systems show poor printing properties due to their delayed network formation. With the addition of a methacrylate to a thiol-yne system the curing rate increases which results in a printable resin with a high monomer conversion.

The 3D printing of bone screws was tested for ternary systems with DPC or DBC as alkyne. Absorbers were added to the systems 0.01 wt% Sudan II. Each layer was illuminated for 30 seconds and the results are displayed in Figure 28 and Figure 29.

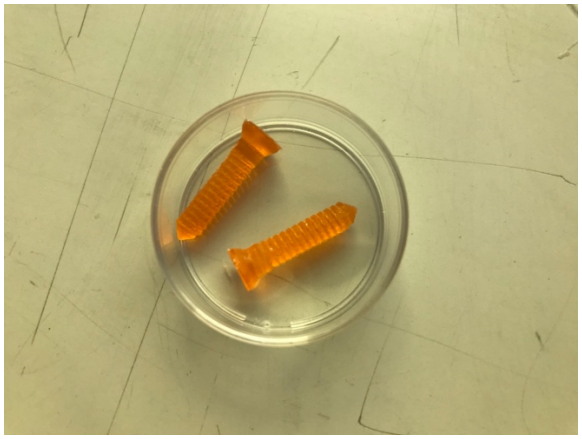

Figure 28 3D printed bone screws from a ternary system containing DBC.

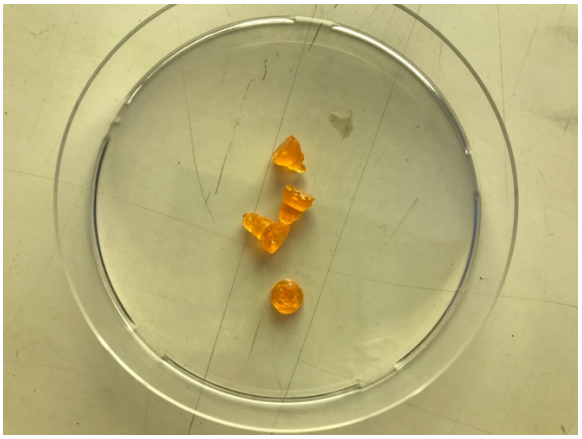

Figure 29 3D printed bone screws from a ternary system containing DPC.

As can be seen, the printing with the ternary system containing DBC lead to defined bone screws. In contrast, the screws with the ternary system containing DPC broke during the printing process and no proper bone screw was obtained with the same printing settings. This is explicable with the slower reactivity of the ternary system with DPC compared to the ternary system with DBC. The DBC-ternary system offers a faster photoreactivity and higher monomer conversion. Therefore, a shorter illumination time can be used to obtain accurate screws.

3.8. Preparation and evaluation of filled resin systems

The filled resin systems can be either used as composite materials or as binder materials for ceramic particles. Since the ternary system only shows sufficient storage stability with the hazardous pyrogallol stabilizer system, it is not possible to use this resin as a binder for composite materials. However, an application as binder material for ceramics is possible because the organic matrix is removed during the sinter process.

After the 3D-printing process the binder material is sintered to yield high-performance ceramics. For this purpose, the ternary system needs to be filled with a high number of ceramic particles. To evaluate the maximum filling degree, the resin was filled with varying concentrations of the ceramic particles and the resulting texture was analyzed via rheometric measurements.

3.8.1. Tricalciumphosphate

The first measurements were carried out with tricalciumphosphate (TCP). TCP is used as a bone-replacement material and, therefore, exhibits excellent biocompatibility.[62]

In the beginning, the first investigations were conducted parallel to the evaluation of the best methacrylate and stabilizer system for the ternary resin. Therefore, all methacrylates were tested for their degree of filling. To obtain a homogeneous slurry, a dispersant from Lithoz was added to the formulation. To achieve the maximum amount of ceramic particles, the resins were filled with a lower concentration of TCP and blended via a two-axis mixer. The two-axis rotation of this mixer allowed uniform homogenization even for materials which were challenging to blend evenly. The concentration of the TCP was increased until no smooth resins could be obtained anymore.

All systems were incorporated with up to 55 wt% of TCP and the system with NPGDMA even up to 65 wt% TCP. The following Figure 30 shows the viscosity of the systems with different temperature settings.

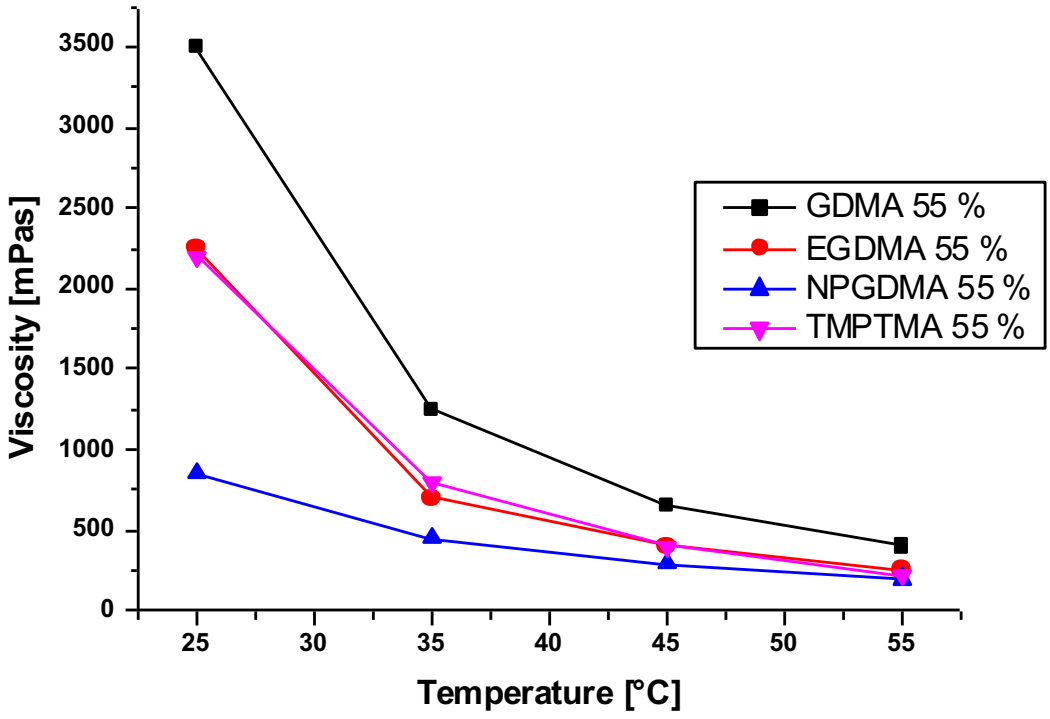

Figure 30 Viscosity of resins filled with 55 wt% TCP at different temperature.

Also, the storage stability of the filled resins systems was investigated at 50 °C. Even though a long stability for the non-filled ternary system was achieved, resins containing TCP could not be stabilized. After one day at 50 °C all samples were cured and could not be measured.

Since a sufficient shelf-life of the dispersion could not be provided, the filling with TCP was not repeated with the final ternary system. A possible explication for the decline in the storage stability could be small amounts of (transition) metals in the TCP powder. These metals are known for their catalytic activity and may have caused the premature polymerization.

3.8.2. Aluminium oxide

Since TCP could not be stabilized, the same procedure was tested with different ceramic particles. Aluminium oxide (Al_2O_3) was selected because of its low content of (transition) metals in the powder. Moreover, it also shows high biocompatibility and can be used in medical engineering for permanent implants or devices. [63]
The degree of filling was solely determined for the final ternary system which is composed according to Table 17.

Table 17 Composition for the Al_2O_3 filled resin.

Thiol	Alkyne	Methacrylate	Radical scavenger	Stabilizer	Photoinitiator
PETMP	DPC	70% NPGDMA + 30% TMPTMA	1% Pyrogallol	4% Miramer A 99	0.5% TPO-L + 2% BAPO

For a homogeneous slurry a dispersant from Lithoz was added to the formulation. The achieved degree of filling for this system was 65%. It was also possible to stabilize this formulation but within one day the homogeneous phases of the resin segregated. This means that the resin needs to be dispersed again for further applications. A possible solution for this problem could be the usage of different dispersants or a more viscous ternary system.

A test sample of the final ternary system filled with 50 wt% Al_2O_3 was 3D-printed at Lithoz and can be seen in Figure 31. The specimen was sintered after the printing process and the parameters are stated in Table 18.

Table 18 Sinter parameter for Al_2O_3 3D-printed device.

Preheating time [h]	Heating rate [K/min]	Holding temperature [°C]	Holding time [h]
		25	
1.01	2.9	200	0
10.00	0.67	600	0
6	1.53	1150	0
9.5	0.88	1650	2
9.00	-0.83	1200	0
10.47	-1.83	50	0

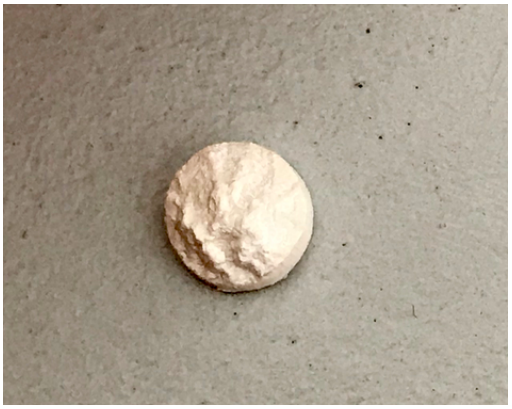

Figure 31 Test 3D-print of a bone screw consisting of a ternary system filled with Al_2O_3.

In the beginning of the printing process the obtained structure looked really promising but over night the whole resin solidified and the printing process stopped. Since the formulation was be stabilized, the premature polymerization of the filled resin was unexpected. Further printing tests should be carried out at Lithoz to determine possible uncertainties.

4. Conclusion and outlook

The aim of this master thesis was the investigation of a new ternary resin which exhibits a fast curing rate, high monomer conversion, low shrinkage stress, and extended storage stability. The resin is used as a binder material for ceramic particles which is sintered after the printing process to yield high-performance ceramics. For example, these ceramics can be applied as bone screws or implants.

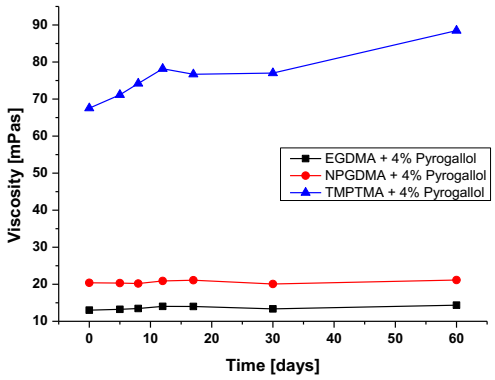

Figure 32 Stabilization of the ternary system with 4% pyrogallol and 4% Miramer A99.

At first, the improvement of the storage stability of the ternary system with different methacrylates was investigated. It was possible to achieve an excellent stabilization of the ternary system for EGDMA, NPGDMA and TMPTMA with 4 mol% pyrogallol and 4 mol% Miramer A99 (Figure 32). Even after 60 days the viscosity increase of the resin with TMPTMA did not exceed 31% and the systems with EGDMA or NPGDMA showed nearly no increase at all. The ternary system with GDPMA as methacrylate exhibited a viscosity increase of about 15000% within eight days and was, therefore, not further considered.

The photoreactivity of all methacrylates were studied via Photo-DSC towards a high monomer conversion and a fast curing speed. The obtained results are summarized in Figure 33 and show that the reactivity of EGDMA was too low for the final ternary system. Even though GDMA showed good monomer conversion and a fast curing rate, it was not further considered because of its poor storage stability. By far the fastest reaction rate was obtained by the ternary system with TMPTMA but the drawback of this methacrylate was its comparably low monomer conversion. NPGDMA featured the most interesting molecule structure but it

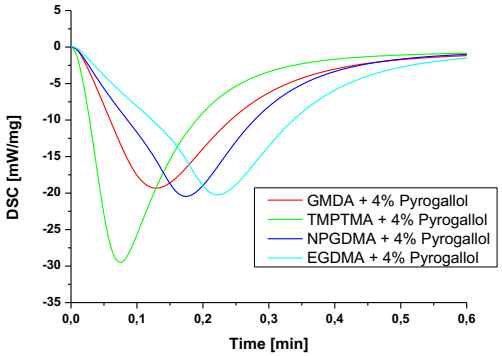

Figure 33 Comparison between the photoreactivity of all tested methacrylates in the ternary system without stabilizer.

exhibited only average results regarding monomer conversion and reaction rate. This lead to the investigation of methacrylate blends containing TMPTMA and NPGDMA.

With the combination of 30% TMPTMA and 70% NPGDMA the best features of both methacrylates were combined.

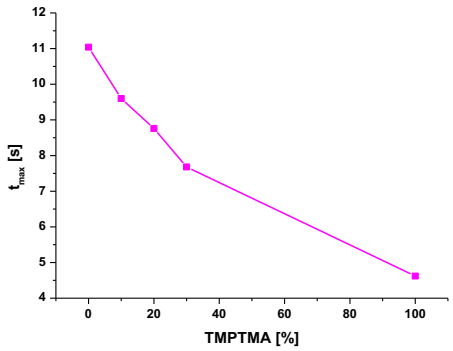

Figure 34 Influence on the reaction rate for increasing TMPTMA concentrations in a ternary system containing 2% BAPO and 0.5% TPO-L.

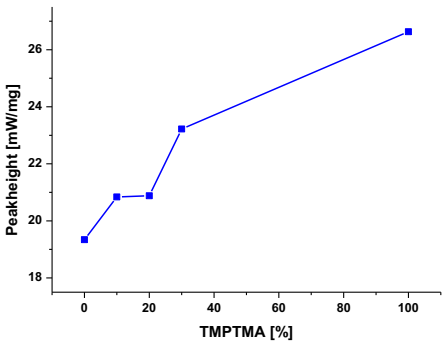

Figure 35 Influence on the peak height for different TMPTMA concentrations in a ternary system containing 2% BAPO and 0.5% TPO-L.

As seen in Figure 34, a decrease in t_{max} of around 44% was obtained with the application of the methacrylate blend compared to a ternary system with only NPGDMA. Furthermore, the peak height decreased (Figure 35) by around 14% and the monomer conversion increased by around 4% compared to a system with solely TMPTMA.

Moreover, the influence of the photoinitator was investigated and 2% BAPO and 0.5% TPO-L showed the best results. Also, the concentration of pyrogallol was studied according to its impact on photoreactiviy. No significant influence on t_{max} was detected but the monomer conversion between 1% and 4% pyrogallol declined by around 18%. Since 1% pyrogallol offered a sufficient stabilization this stabilizer concentration was used for the ternary system.

Furthermore, the monomer conversion of a pure methacrylate system containing 30% TMPTMA/70% NPGDMA and a ternary system containing the same methacrylate blend with different alkynes was studied. The analysis indicated that the pure methacrylate system showed the least monomer conversion of all samples tested. (Figure 36) Even after post-curing no apparent increase in monomer conversion was noticeable. The ternary system containing DPC showed a lower methacrylate conversion (45%) compared to the ternary system

containing DBC (68%). After post-curing both ternary systems showed a higher methacrylate conversion. The resin with DPC exhibited an increase in methacrylate conversion from 45% to 64%, whereas the system with DBC showed an increase from 68% to 78%.

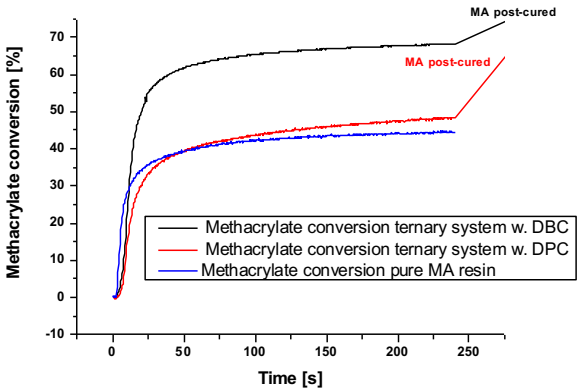

Figure 36 Methacrylate conversion in different ternary resin systems.

The cured ternary systems containing the methacrylate blend and either DPC or DBC as alkyne were investigated towards their migration of the monomers. The analysis showed that only a low migration of the alkynes could be identified. The used methacrylates did not migrate and could not be detected.

For the analysis of the impact strength and HDT, plates containing the pure methacrylate-blend and a ternary system with the methacrylate-blend and DPC or DBC as alkyne were produced. Only the plates with the ternary system could be cut into the desired rods for the analysis since the pure methacrylate plate cracked during the curing process. (Figure 39) The cracking of the plate was probably caused by the experience of shrinkage stress during the illumination. The obtain impact strength for DBC (5 kJ/m^2) and DPC (2 kJ/m^2) indicated rather brittle properties. The HDT for the DBC-system was obtained as 171.3 °C and for DPC-system 117.2 °C.

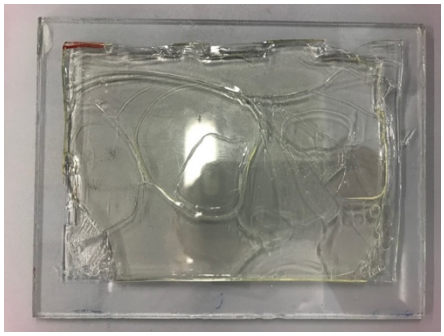

Figure 37 Pure methacrylate plate for charpy impact and HDT measurements after curing.

Furthermore, the 3D printing of medical devices was attempted. As seen in Figure 38, with the ternary system containing DBC and 0.01% Sudan II defined bone screws were obtained. The ternary system with DPC broke off during the printing system and therefore no screws could be achieved.

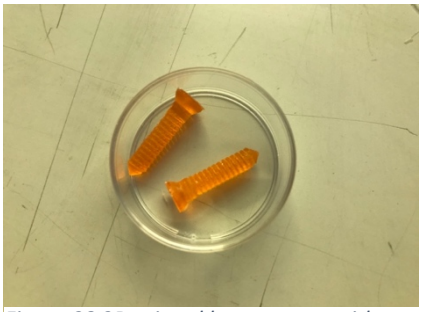

Figure 38 3D printed bone screws with a ternary system containing DBC.

Furthermore, for each methacrylate the maximum content of TCP particles was investigated.

Figure 39 Test 3D-print of a bone screw consisting of a ternary system filled with Al_2O_3.

For TCP, a maximum filling degree of 55 wt% respectively 65 wt% for NPGDMA could be obtained. The subsequent storage stability tests lead to the result that a stabilization of the filled resin system with TCP was not possible. This could be explicable with the presence of (transition) metals in the TCP powder which are known for their catalytic activity. Since the TCP formulation further storage stability tests for the final ternary system have not been carried out.

Al_2O_3 was selected as a possible alternative for TCP. A maximum filling degree for the final ternary of 65% was achievable. It was possible to stabilize a resin filled with 50 wt% for several days but the homogeneous dispersion segregated after one day. A test specimen of the ternary resin filled with Al_2O_3 was printed at Lithoz (Figure 37). The resin solidified over night and the printing process could not be finished. The obtained specimen was sintered.

Further investigations are needed concerning the storage stability of the ternary resin. Even though an efficient stabilizer system was provided with pyrogallol and Miramer A99, research towards a less cytotoxic alternative should be carried out. This could increase the range of possible applications for the ternary system, e.g. in composite materials.

Moreover, an efficient stabilizer system for the filled resins need to be developed. A promising stabilizer system for ternary systems is currently under group-intern research, which could also provide enhancement in the storage stability of filled resins.

5. Experimental

5.1. Synthesis

5.1.1. Synthesis of di(prop-2-yn-1-yl) carbonate (1)

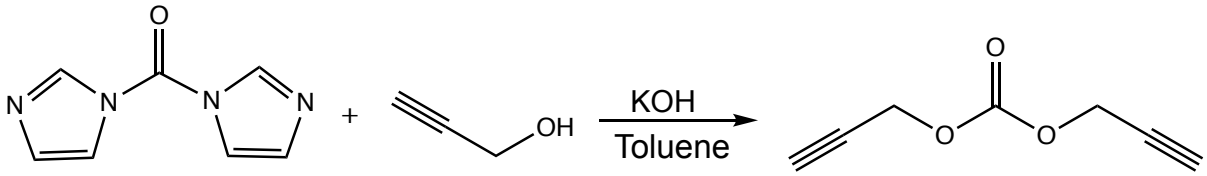

Scheme 11 Synthesis of DPC

Into a suspension of 1,1'-Carbonyldiimidazole (600 g, 3.7 mol, 1.0 equiv.) in 500 mL abs. toluene 2-Propyn-1-ol (622 g, 11.1 mol, 3.0 equiv.) is added dropwise and the reaction mixture is allowed to stirr over night at room temperature. Subsequently the toluene is removed under reduced pressure. Afterwards distilled water is added and the solution is extracted three times with dichloromethane. The combined organic layers are dried over Na_2SO_4 and the solvent is evaporated under reduced pressure. Finally, the remaining yellowish solution is distilled to yield the product as a clear liquid. (89 %, 454 g)

1H-NMR: (δ, 400 MHz, 25 °C, $CDCl_3$):

4.92 (d, J = 2.5 Hz, 4H, CH_2), 3.28 (t, J = 2.5 Hz, 4H, CH) ppm.

13C-NMR: (δ, 400 MHz, 25 °C, $CDCl_3$):

153.20 (1C, C=O); 80.16 (2C, C); 74.18 (2C, CH); 55.34 (2C, CH_2) ppm.

5.1.2. Synthesis of di(but-3-yn-1-yl) carbonate (2)

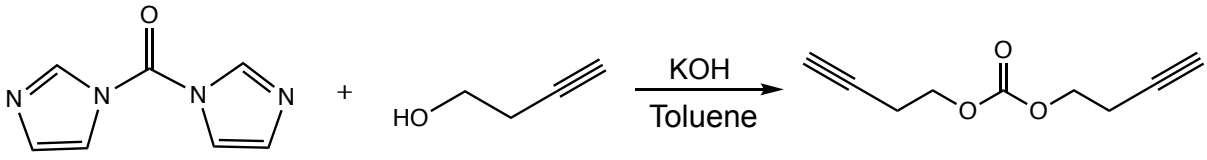

Scheme 12 Synthesis of DBC

Into a suspension of 1,1'-Carbonyldiimidazole (600 g, 3.7 mol, 1.0 equiv.) in 500 mL abs. toluene 3-Butyn-1-ol (778 g, 11.1 mol, 3.0 equiv.) is added dropwise and the reaction mixture is allowed to stirr over night at room temperature. Subsequently the toluene is removed under

reduced pressure. Afterwards distilled water is added and the solution is extracted three times with dichloromethane. The combined organic layers are dried over Na_2SO_4 and the solvent is evaporated under reduced pressure. Finally, the remaining yellowish solution is distilled to yield the product as a clear liquid. (91 %, 559.12 g)

1H-NMR: (δ, 400 MHz, 25 °C, $CDCl_3$):

4.84 (t, J = 2.7 Hz, 4H, CH_2), 2.91 (t, J = 2.6 Hz, 2H, CH), 2.29 (t, J = 2.7 Hz, 4H, CH_2) ppm.

13C-NMR: (δ, 400 MHz, 25 °C, $CDCl_3$):

154.81 (1C, C=O); 80.98 (2C, C); 70.63 (2C, CH); 64.72 (2C, CH_2); 18.34 (2C, CH_2) ppm.

5.2. Methods and equipment

5.2.1. ^{1}H-NMR spectroscopy

^{1}H NMR was performed on a Varian 400-NMR spectrometer operating at 399.66 MHz respectively. A relaxation delay of 10 s and a 45° pulse were used for acquisition of the ^{1}H- and ^{13}C-NMR spectra.

5.2.2. Photo differential scanning calorimetry (DSC)

The Photo-DSC measurements were performed on a NETZSCH Photo-DSC 204 F1 Phoenix. All measurements were conducted at 50 °C in aluminium crucibles under nitrogen flow (20 $mL*min^{-1}$). Each measurement was carried out with 8 ± 0.5 mg of sample. As a light source an Omnicure s2000 UV-Lamp was used at 1 $W*cm^{-2}$. For the determination of the reaction enthalpy and t_{max}, the samples were illuminated twice for 10 minutes each with an idle time of 2 minutes in between. For the analysis, the second measurement was abstracted from the first one to yield a reaction enthalpy curve. The enthalpy was determined from the peak area.

5.2.3. Vortex two-axis centrifugal mixer

The resins were homogenized with a Vortex Mixer VM-200 purchased from StateMix (Winnipeg, Canada).

5.2.4. UV-curing belt “Lighthammer”

For the curing of the specimens a UV-curing system from Heraeus Noblelight (Gaithersburg, USA) was used. The curing was conducted with a lowpressure mercury-vapor lamp and the required intensity and belt velocity justified according to Table 19.

Table 19 Paramters of UV-curing and the resulting power

Intensity [%]	**Belt velocity [m/min]**	**Power [mW/cm^2]**
25	8	55
40	4	323

5.2.5. Post-curing device

The post-curing device consists of 4 LEDs with an adjustable z-axis. The emission maximum is at 405 nm and the temperature is regulated with a hot plate. For the post-curing the sample is placed between two glass plates and heated to 100 °C. The curing takes place at 405 nm for 30 minutes for each side of the specimen.

5.2.6. Rheometer

The viscosity was determined on a Modular Compact Rheometer MCR 102 from Anton Paar (Graz, Austria) with a CP60-0.5/TI cone (diameter 60 mm and opening angle 0,5°). For each measurement approximately 1 ml of the sample was used and the parameters were set to 25 °C and 300^{1-s} shear rate.

5.2.7. GC-MS

GC-MS analysis of the ethanol extracts of the samples was performed using a GCMS-QP2010 Plus from SHIMADZU (Nakagyo-ku, Japan) equipped with a Optima-5-Accent column (30 m x 0.25 µm x 0.25 µm) and an AOC-20i Auto injector. As carrier gas He was used and the following settings (Table 20) were applied:

Table 20 GC-MS parameters

Column Oven T [°C]	35

Injection T [°C]	250
Injection Mode	Split
Flow Control Mode	Linear Velocity
Pressure [kPa]	35.3
Total Flow [mL/min]	146.6
Column Flow [mL/min]	0.84
Linear Velocity [cm/sec]	33
Purge Flow [mL/min]	3
Split Ratio	170

5.2.8. Fourier transformed infrared spectroscopy (FTIR)

FTIR measurements were conducted on a VERTEX 70 (Bruker, Billerica, USA) in reflection mode with the unit A513. 1µl of the sample was placed between two CaF_2 plates (8 mm diameter, 1 mm thickness) and illuminated with an Omnicure s1000 (Lumen Dynamics, Mississauga, USA) at 100 % intensity (436 mW/cm^2) with a 9 cm gap between sample and light. Right after the measurements, the samples were post-cured thermally at 100 °C for 15 minutes with the UV-curing belt "Lighthammer" and illuminated again.

5.2.9. mUVe 3D DLP printer

The 3D printer is based on digital light processing (DLP) and was purchased from mUVe 3D (Grand Rapids, USA). As lightsource a ViewSonic projector (1920 x 1080 pixel) was used which was placed underneath a transparent resin container. Above the container a moving platform is installed where the printed specimens adhered to. Each layer was cured for 30 s to yield a layer thickness of 100 µm.

5.2.10. Charpy Impact Test

The determination of the impact strength was carried out on a CEAST RESIL 25. The samples were cut in 80 x 5 x 2 mm specimens with a diamond blade and were applied planar to the counterfort. The used pendulum was set to an impact energy of 0.5 J and all measurements were carried out at room temperature.

5.3. Reagents

All reagents were purchased from TCI, VWR International, Bruno Bock chemische Fabrik GmbH & Co. KG, BASF or Sigma Aldrich. The composite material (TCP and Al_2O_3) and the dispersive agents were provided by Lithoz. All reagents were used without further purification unless stated otherwise.

6. Appendix

6.1. List of Abbreviations

Three-dimensional	3D
Additive manufacturing technologies	AMT
Bis-acylphosphine oxide	BAPO
Di(But-3-yn-1-yl) carbonate	DBC
Digital light processing	DLP
Di(Prop-2-yn-1-yl) carbonate	DPC
Differential scanning calorimetry	DSC
Ethylen glycol dimethacrylate	EGDMA
Gas chromatography-mass spectrometry	GC-MS
Glycerol dimethacrylate	GDMA
Heat deflection temperature	HDT
Nuclear magnetic resonance	NMR
Neopentyl glycol dimethacrylate	NPGDMA
Pentaerythitol tetra(3-mercaptopropionat)	PETMP
Parts per million	ppm
Tricalciumphosphate	TCP
Glass transition temperature	T_g
Trimethylolpropan trimethacrylate	TMPTMA
Ethyl(2,4,6-trimethylbenzoyl)phenylphosphinate	TPO-L

6.2. List of Figures

6.3. List of Schemes

6.4. List of Tables

6.5. References

[1] B. Husár, R. Liska, *Chem. Soc. Rev.* **2012**, *41*, 2395–2405.
[2] T. Wohlers, *Wohlers Report 2015: 3D Printing and Additive Manufacturing State of Industry*, **2015**.
[3] L. E. Murr, E. Martinez, K. N. Amato, S. M. Gaytan, J. Hernandez, D. A. Ramirez, P. W. Shindo, F. Medina, R. B. Wicker, *J. Mater. Res. Technol.* **2012**, *1*, 42–54.
[4] D. L. Bourell, *Met. Powder Rep.* **1993**, *48*, 47.
[5] A. Zocca, P. Colombo, C. M. Gomes, J. Günster, *J. Am. Ceram. Soc.* **2015**, *98*, 1983–2001.
[6] J. N.-M. L. Novakova-Marcincinova, *Appl. Mech. Mater* **2013**, *309*, 133–140.
[7] M. Pavan, T. Craeghs, R. Verhelst, O. Ducatteeuw, J. P. Kruth, W. Dewulf, *Case Stud. Nondestruct. Test. Eval.* **2016**, *6*, 62–68.
[8] H. N. Chia, B. M. Wu, *J. Biol. Eng.* **2015**, *9*, 1–14.
[9] S. C. Ligon-Auer, M. Schwentenwein, C. Gorsche, J. Stampfl, R. Liska, *Polym. Chem.* **2016**, *7*, 257–286.
[10] C. Gorsche, K. Seidler, P. Knaack, P. Dorfinger, T. Koch, J. Stampfl, N. Moszner, R. Liska, *Polym. Chem.* **2016**, *7*, 2009–2014.
[11] R. Felzmann, S. Gruber, G. Mitteramskogler, P. Tesavibul, A. R. Boccaccini, R. Liska, J. Stampfl, *Adv. Eng. Mater.* **2012**, *14*, 1052–1058.
[12] M. Schwentenwein, J. Homa, *Int. J. Appl. Ceram. Technol.* **2015**, *12*, 1–7.
[13] J. R. Tumbleston, D. Shirvanyants, N. Ermoshkin, R. Janusziewicz, A. R. Johnson, D. Kelly, K. Chen, R. Pinschmidt, J. P. Rolland, A. Ermoshkin, et al., **2015**, *347*, 635–639.
[14] A. M. . Greenberg, J. Prein, *Craniomaxillofacial Reconstructive and Correvtive Bone Surgery*, Springer Verlag New York, **2002**.
[15] B. Bhushan, M. Caspers, *Microsyst. Technol.* **2017**, *23*, 1117–1124.
[16] D. P. Mukherjee, W. S. Pietrzak, *J. Craniofac. Surg.* **2011**, *22*, 679—689.
[17] S. Li, **1999**, 342–353.
[18] R. M. Laughlin, M. S. Block, R. Wilk, R. B. Malloy, J. N. Kent, *J. Oral Maxillofac. Surg.* **2007**, *65*, 89–96.
[19] Y. Shikinami, M. Okuno, *Biomaterials* **2001**, *22*, 3197–3211.
[20] M. Schuster, C. Turecek, B. Kaiser, J. Stampfl, R. Liska, F. Varga, *J. Macromol. Sci. Part A* **2007**, *44*, 547–557.
[21] A. Oesterreicher, J. Wiener, M. Roth, A. Moser, R. Gmeiner, M. Edler, G. Pinter, T. Griesser, *Polym. Chem.* **2016**, *7*, 5169–5180.
[22] C. D. Calnan, *Contact Dermatitis* **1980**, 6.
[23] J. . Andrews, L.S. Clary, *J. Toxikol. Environ. Heal.* **1986**, *19*, 149–164.
[24] M. Friedman, J. F. Cavins, J. S. Wall, *J. Am. Chem. Soc.* **1965**, *87*, 3672–3682.
[25] N. Moszner, U. Salz, *Macromol. Mater. Eng.* **2007**, *292*, 245–271.
[26] D. Karalekas, A. Aggelopoulos, *J. Mater. Process. Technol.* **2003**, *136*, 146–150.
[27] A. Oesterreicher, G. Christian, S. Ayular-Karunakaran, A. Moser, M. Edler, G. Pinter, S. Sandra, L. Robert, T. Griesser, *Macromol. Rapid Commun.* **2016**, *37*, 1701–1706.
[28] A. Oesterreicher, S. Ayalur-Karunakaran, A. Moser, F. H. Mostegel, M. Edler, P. Kaschnitz, G. Pinter, G. Trimmel, S. Schlögl, T. Griesser, *J. Polym. Sci. Part A Polym.*

Chem. **2016**, *54*, 3484–3494.
[29] C. N. Bowman, C. J. Kloxin, *AlChE* **2008**, *54*, 2775–2795.
[30] C. E. Hoyle, T. Y. Lee, T. Roper, *J. Polym. Sci. Part A Polym. Chem.* **2004**, *42*, 5301–5338.
[31] S. Ye, N. B. Cramer, I. R. Smith, K. R. Voight, C. N. Bowman, *Macromolecules* **2011**, *44*, 9084–9090.
[32] S. K. Reddy, N. B. Cramer, C. N. Bowman, *Macromolecules* **2006**, *39*, 3681–3687.
[33] T. Y. Lee, J. Carioscia, Z. Smith, C. N. Bowman, *Macromolecules* **2007**, *40*, 1473–1479.
[34] B. . Fairbanks, E. . Sims, K. S. Anseth, C. N. Bowman, *Macromolecules* **2010**, *43*, 4113–4119.
[35] S. Parker, R. Reit, H. Abitz, G. Ellson, K. Yang, B. Lund, W. E. Voit, *Macromol. Rapid Commun.* **2016**, *37*, 1027–1032.
[36] N. B. Cramer, C. N. Bowman, *Polym. Chem.* **2001**, *39*, 3311–3319.
[37] J. W. Chan, C. E. Hoyle, A. B. Lowe, M. Bowman, *Macromolecules* **2010**, *43*, 6381–6388.
[38] J. W. Chan, H. Zhou, C. E. Hoyle, A. B. Lowe, *Chem. Mater.* **2009**, *21*, 1579–1585.
[39] M. Edler, F. H. Mostegel, M. Roth, A. Oesterreicher, S. Kappaun, T. Griesser, *J. Appl. Polym. Sci.* **2017**, *134*, 1–7.
[40] P. Esfandiari, S. C. Ligon, J. J. Lagref, R. Frantz, Z. Cherkaoui, R. Liska, *J. Polym. Sci. Part A Polym. Chem.* **2013**, *51*, 4261–4266.
[41] E. Klemm, S. Sensfuss, U. Holfter, H. J. Flammersheim, *Angew. Makromol. Chem.* **1993**, 121–127.
[42] G. Kuhne, J. S. Diesen, E. Klemm, *Angew. Makromol. Chem.* **1996**, 139–145.
[43] V. R. Preedy, H. Abramovic, *Coffee in Health and Disease Prevention*, Academic Press, London, **2014**.
[44] N. . Mankovich, D. Samson, W. Pratt, D. Lew, J. Beumer, *Otolaryngol. Clin. North Am.* **1994**, *27*, 875–889.
[45] A. Curodeau, E. Sachs, S. Caldarise, *J. Biomed. Mater. Res.* **2000**, *53*, 525–535.
[46] B. C. Gross, J. L. Erkal, S. Y. Lockwood, C. Chen, D. M. Spence, *Anal. Chem.* **2014**, *86*, 3240–3253.
[47] F. P. W. Melchels, J. Feijen, D. W. Grijpma, *Biomaterials* **2010**, *31*, 6121–6130.
[48] U. Meyer, H.-P. Wiesmann, *Head Face Med.* **2005**, *1*, 2.
[49] F. J. O'Brien, *Mater. Today* **2011**, *14*, 88–95.
[50] E. Vorndran, M. Klarner, U. Klammert, L. M. Grover, S. Patel, J. E. Barralet, U. Gbureck, *Adv. Eng. Mater.* **2008**, *10*, 67–71.
[51] S. Bose, S. Vahabzadeh, A. Bandyopadhyay, *Mater. Today* **2013**, *16*, 496–504.
[52] M. Pfaffinger, M. Hartmann, M. Schwentenwein, J. Stampfl, *Int. J. Appl. Ceram. Technol.* **2017**, *14*, 499–506.
[53] M. Schwentenwein, P. Schneider, J. Homa, *Adv. Sci. Technol.* **2014**, *88*, 60–64.
[54] M. L. Griffith, J. W. Halloran, *J. Am. Ceram. Soc.* **1996**, *79*, 2601–2608.
[55] C.-J. Bae, J. Halloran, *Int. J. Appl. Ceram. Technol.* **2011**, *8*, 1289–1295.
[56] "Photo DSC," can be found under https://www.netzsch-thermal-analysis.com/en/products- solutions/differential-scanning-calorimetry/dsc-214-polyma/., **n.d.**
[57] G. D. B. B. Palova Santos Balzer, José Henrique Vieira Maia, Claudio Lucas Kochhann, *Gel with Compatibilizing Agents Based on Silane, EGDMA Polymer Matrix Involving Glass Fibers for Reinforcement in Acrylic Resin and Appropriate Method of Application in Dentistry*, **2016**.

[58] S. Gmbh, *Verordnung Über Die Zulassung von Zusatzstoffen Zu Lebensmitteln Zu Technologischen Zwecken (Zusatzstoff-Zulassungsverodnung - ZZulV)*, **2012**.
[59] G. Russmueller, R. Liska, J. Stampfl, C. Heller, A. Mautner, K. Macfelda, B. Kapeller, R. Lieber, A. Haider, K. Mika, et al., *Materials (Basel).* **2015**, *8*, 3685–3700.
[60] Y. Muzukami, *Kyushu Shika Gakkai Zasshi* **1986**, *40*, 807–35.
[61] M. Worzakowska, *J. Therm. Anal. Calorim.* **2018**, *132*, 225–232.
[62] K. Köster, E. Karbe, H. Kramer, H. Heide, R. König, *Langenbecks Arch. Chir.* **1976**, *341*, 77–86.
[63] *Riction, Lubrication and Wear Technology*, **1992**.